beta protein potently inhibit hippocampal long-term potentiation in vivo. Nature 416, 535–539.
[17] Scott, H.L., Tannenberg, A.E.G. and Dodd, P.R. (1995) Variant forms of neuronal glutamate transporter sites in Alzheimer disease cerebral cortex. J. Neurochem. 64, 2193–2202.
[18] Robinson, M.B. (1999) The family of sodium-dependent glutamate transporters: a focus on the GLT-1/EAAT2 subtype. Neurochem. Int. 33, 479–491.
[19] Arriza, J.L., Fairman, W.A., Wadiche, J.I., Murdoch, G.H., Kavanaugh, M.P. and Amara, S.G. (1994) Functional comparisons of three glutamate transporter subtypes cloned from human motor cortex. J. Neurosci. 14, 5559–5569.
[20] Dong, X.X., Wang, Y. and Qin, Z.H. (2009) Molecular mechanisms of excitotoxicity and their relevance to pathogenesis of neurodegenerative diseases. Acta Pharmacol. Sin. 30, 379–387.
[21] Tanaka, K. et al. (1997) Epilepsy and exacerbation of brain injury in mice lacking the glutamate transporter GLT-1. Science 276, 1699–1702.
[22] Masliah, E. et al. (1996) Deficient glutamate transport is associated with neurodegeneration in Alzheimer's disease. Ann. Neurol. 40, 759–766.
[23] Scott, H.L., Pow, D.V., Tannenberg, A.E. and Dodd, P.R. (2002) Aberrant expression of the glutamate transporter excitatory amino acid transporter 1 (EAAT1) in Alzheimer's disease. J. Neurosci. 22, RC206.
[24] Thai, D.R. (2002) Excitatory amino acid transporter EAAT-2 in tangle-bearing neurons in Alzheimer's disease. Brain Pathol. 12, 405–411.

nature genetics

LETTERS

Genome-wide association study identifies common variants at four loci as genetic risk factors for Parkinson's disease

Wataru Satake[1–3], Yuko Nakabayashi[1,2], Ikuko Mizuta[1,2], Yushi Hirota[1,2], Chiyomi Ito[1,2], Michiaki Kubo[4], Takahisa Kawaguchi[4], Tatsuhiko Tsunoda[4], Masahiko Watanabe[5], Atsushi Takeda[6], Hiroyuki Tomiyama[7], Kenji Nakashima[8], Kazuko Hasegawa[9], Fumiya Obata[10], Takeo Yoshikawa[11], Hideshi Kawakami[12], Saburo Sakoda[3], Mitsutoshi Yamamoto[13], Nobutaka Hattori[7], Miho Murata[14], Yusuke Nakamura[4,15] & Tatsushi Toda[1,2]

To identify susceptibility variants for Parkinson's disease (PD), we performed a genome-wide association study (GWAS) and two replication studies in a total of 2,011 cases and 18,381 controls from Japan. We identified a new susceptibility locus on 1q32 ($P = 1.52 \times 10^{-12}$) and designated this as *PARK16*, and we also identified *BST1* on 4p15 as a second new risk locus ($P = 3.94 \times 10^{-9}$). We also detected strong associations at *SNCA* on 4q22 ($P = 7.35 \times 10^{-17}$) and *LRRK2* on 12q12 ($P = 2.72 \times 10^{-8}$), both of which are implicated in autosomal dominant forms of parkinsonism. By comparing results of a GWAS performed on individuals of European ancestry, we identified *PARK16*, *SNCA* and *LRRK2* as shared risk loci for PD and *BST1* and *MAPT* as loci showing population differences. Our results identify two new PD susceptibility loci, show involvement of autosomal dominant parkinsonism loci in typical PD and suggest that population differences contribute to genetic heterogeneity in PD.

Parkinson's disease (MIM168600) is one of the most common neurodegenerative diseases worldwide, affecting 1–2% of individuals aged ≥65 years[1]. Clinical features of PD result primarily from loss of dopaminergic neurons in the substantia nigra. Various medical treatments improve PD symptoms but do little to deter disease progression. Identifying genetic risk factors for PD will be helpful in elucidating the pathogenesis of the disease. Linkage studies have been successful in mapping genes for mendelian forms of parkinsonism: *SNCA* (encoding α-synuclein)[2] and *LRRK2* (refs. 3,4) in autosomal dominant forms, and *PARK2* (encoding parkin), *PINK1*, *PARK7* (encoding DJ-1) and *ATP13A2* in autosomal recessive forms[5,6]. However, mendelian forms of parkinsonism are rare compared to the far more common typical PD, a complex disorder caused by multiple genetic and environmental factors[7]. Association studies have evaluated variants in many candidate genes for PD[7], but only a few, such as common variants of *SNCA*[8–10] and rare mutations of *GBA*[11], have been identified as PD-susceptibility genes with genome-wide significance. Recently, GWASs in PD have provided association evidence at several loci, but not at the genome-wide significant level[12–14].

We conducted a GWAS and two subsequent replication studies for PD to identify further common variants that contribute to disease. In the GWAS stage, we genotyped 561,288 SNPs on autosomal and sex chromosomes using the HumanHap550 array (Illumina). The GWAS stage included 1,078 PD cases and 2,628 controls in the Japanese population (**Supplementary Note**). After SNP and sample quality control analyses, we used genotype data from 435,470 SNPs in 988 cases and 2,521 controls in the GWAS analysis (see Online Methods).

We tested for association between each SNP and PD using the Cochran-Armitage trend test with 1 d.f. The quantile-quantile plot showed a close match to test statistics expected under the null distribution (genomic inflation factor $\lambda = 1.055$ for PD) (**Fig. 1a,b**). This indicates minimal overall inflation of genome-wide statistical results due to population stratification and also reveals a number of SNPs whose *P* values exceed those expected under the null hypothesis. Seventeen SNPs showed $P < 5 \times 10^{-7}$, the threshold for genome-wide significance suggested by the Wellcome Trust Case Control Consortium[15] (**Fig. 1c**). All these SNPs were located on 4q22, a region harboring *SNCA* that was previously identified by us and others as a definite susceptibility gene for PD[8–10].

[1]Division of Neurology/Molecular Brain Science, Kobe University Graduate School of Medicine, Kobe, Japan. [2]Division of Clinical Genetics, Osaka University Graduate School of Medicine, Suita, Japan. [3]Department of Neurology, Osaka University Graduate School of Medicine, Suita, Japan. [4]Center for Genomic Medicine, RIKEN, Yokohama, Japan. [5]Department of Neurology, Graduate School of Comprehensive Human Sciences, University of Tsukuba, Tsukuba, Japan. [6]Division of Neurology, Tohoku University Graduate School of Medicine, Sendai, Japan. [7]Department of Neurology, Juntendo University School of Medicine, Tokyo, Japan. [8]Department of Neurology, Tottori University Faculty of Medicine, Yonago, Japan. [9]Department of Neurology, Sagamihara National Hospital, Sagamihara, Japan. [10]Division of Clinical Immunology, Graduate School of Medical Sciences, Kitasato University, Sagamihara, Japan. [11]RIKEN Brain Science Institute, Saitama, Japan. [12]Department of Epidemiology, Research Institute for Radiation Biology and Medicine, Hiroshima University, Hiroshima, Japan. [13]Department of Neurology, Kagawa Prefectural Central Hospital, Takamatsu, Japan. [14]Department of Neurology, National Center Hospital of Neurology and Psychiatry, Kodaira, Japan. [15]Human Genome Center, Institute of Medical Science, University of Tokyo, Tokyo, Japan. Correspondence should be addressed to T.Toda (toda@med.kobe-u.ac.jp).

Received 5 June; accepted 21 October; published online 15 November 2009; doi:10.1038/ng.485

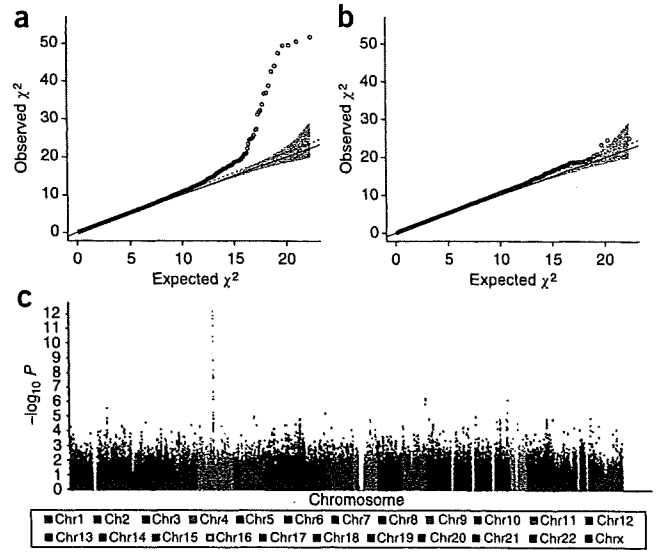

Figure 1 Genome-wide association results from the discovery phase. (**a**) Quantile-quantile plot for test statistics (Cochran-Armitage trend test) for 435,470 SNPs passing quality control. The solid line represents concordance of observed and expected values. Slope of the dashed line represents the genomic inflation factor ($\lambda = 1.055$). The shaded region is the 95% concentration band formed by calculating, for each order statistic, the 2.5th and 97.5th percentiles of the respective distribution under the null hypothesis. (**b**) Quantile-quantile plot for test statistics (Cochran-Armitage trend test) after the removal of the four loci with strong associations in this study (1q32, 4p15, 4q22 and 12q12). (**c**) Manhattan plot presenting the *P* values across the genome. The $-\log_{10} P$ (Cochran-Armitage trend test) from 435,470 SNPs in 988 Parkinson's disease cases and 2,521 controls is plotted according to its physical position on successive chromosomes.

For fast-track replication, we selected the 337 most associated SNPs ($P \leq 0.000533$) from analysis of GWAS data and genotyped them in a sample set of replication 1, which consisted of 612 cases and 14,139 controls from Japan (**Supplementary Note**). Thirty-two SNPs showed association of $P < 0.05$ in replication 1 (**Supplementary Fig. 1**). Combined analyses of the GWAS and replication 1 showed that 12 SNPs in 3 loci (1q32, 4p15 and 4q22) surpassed $P < 5 \times 10^{-7}$. Furthermore, we found association signals ($P = 3.06 \times 10^{-6}$, OR = 1.36) on 12q12, harboring *LRRK2*, which is a causative gene for autosomal dominant parkinsonism (**Table 1**).

In replication 2, we tested 24 SNPs at these four loci for association with PD. An independent sample set (321 cases and 1,614 controls) recruited from Japan was used in replication 2 (**Supplementary Note**). Association evidence was again found at these four loci: 1q32, $P = 2.80 \times 10^{-4}$, OR = 1.37; 4p15, $P = 7.70 \times 10^{-3}$, OR = 1.26; 4q22, $P = 0.02$, OR = 1.22; and 12q12, $P = 6.43 \times 10^{-4}$, OR = 1.57 (**Table 1**). The disease associations on 1q32 and 12q12 exceeded the conservative Bonferroni-corrected threshold for significance ($P = 0.0021$; calculated as 0.05/24). All the SNPs showed allele frequency differences in the same direction in the GWAS, replication 1 and replication 2. Furthermore, combined analysis of the GWAS and two replication stages provided strong evidence of association in the four regions with a significance level of $P = 2.72 \times 10^{-8}$ or less (**Table 1**).

We identified two new susceptibility loci with genome-wide significance on 1q32 and 4p15, which have not been reported to be associated with PD in previous studies[12–14]. On 1q32, seven SNPs (rs16856139, rs823128, rs823122, rs947211, rs823156, rs708730 and rs11240572) reached $P < 5 \times 10^{-7}$ in the overall analysis (**Fig. 2a**). rs947211 showed the strongest association to PD ($P = 1.52 \times 10^{-12}$, OR = 1.30) and is located 8.5 kb upstream of *RAB7L1* and 5.6 kb downstream of *SLC41A1*. Linkage disequilibrium (LD) analysis revealed that SNPs with significant associations to PD lie within several LD blocks containing the following five genes: *SLC45A3*, *NUCKS1*, *RAB7L1*, *SLC41A1* and *PM20D1* (also called *FLJ32569*) (**Table 1** and **Fig. 2a**). Three genes (*NUCKS1*, *RAB7L1* and *SLC41A1*) were contained in the same LD block as rs947211. rs947211 was weakly correlated with the other six SNPs ($r^2 = 0.07$–0.25), and we observed residual association signals when rs947211 and each of the other six SNPs were paired in conditional analyses of our overall data. This result suggests that this locus has multiple independent association signals (**Supplementary Table 1**). These data provide the first evidence, to our knowledge, of an association between 1q32 and PD susceptibility, and we designated this region as *PARK16*.

On 4p15, four SNPs (rs11931532, rs12645693, rs4698412 and rs4538475) reached $P < 5 \times 10^{-7}$ in the combined analysis (**Fig. 2b**). These four SNPs showed strong disease association with almost the same significance levels (ranging from $P = 3.94 \times 10^{-9}$ to $P = 1.78 \times 10^{-8}$, all OR = 1.24); among them, rs4538475 was the most strongly associated. The four SNPs were located from intron 8 to 4.1 kb downstream of *BST1* (bone marrow stromal cell antigen). LD analysis revealed that the four SNPs were correlated with $r^2 > 0.78$ and lie within a 15 kb LD block containing a single gene, *BST1*.

The remaining two intervals (4q22 and 12q12) harbored genes previously found to be causal for autosomal dominant forms of parkinsonism, specifically, *SNCA* and *LRRK2*, respectively. On 4q22, seven SNPs (rs3733449, rs11931074, rs3857059, rs2736990, rs3796661, rs6532194 and rs12233759) throughout the *SNCA* region showed genome-wide significant association in the combined analysis (**Fig. 2c**). The most significantly associated SNPs, rs11931074 ($P = 7.35 \times 10^{-17}$, OR = 1.37) and rs3857059 ($P = 5.68 \times 10^{-16}$, OR = 1.36), are approximately 35.7 kb apart, located 7.2 kb downstream from and in intron 4 of *SNCA*, respectively. The entire *SNCA* gene was divided into two LD blocks at intron 4. Both SNPs were positioned on the 3′ side of the LD block and showed a high degree of LD ($r^2 = 0.98$). Three SNPs (rs2736990, rs3796661 and rs6532194) were moderately correlated with rs11931074 ($r^2 = 0.81$, 0.76 and 0.63, respectively). The remaining two SNPs (rs3733449 and rs12233759) were weakly correlated with rs11931074 ($r^2 = 0.05$ and 0.24, respectively), and residual association signals were marginally observed when rs11931074 and each of these two SNPs were paired in conditional analyses of our overall data (**Supplementary Table 1**). These data confirm *SNCA* as a susceptibility gene for PD.

On 12q12, five SNPs (rs1994090, rs7304279, rs4768212, rs2708453 and rs2046932) surpassed $P < 5 \times 10^{-7}$ in the overall analysis (**Fig. 2d**). The five SNPs showed strong disease association with almost the same significance (ranging from $P = 2.72 \times 10^{-8}$ to $P = 1.09 \times 10^{-7}$, OR = 1.37–1.39); among them, rs1994090 was the most strongly associated to PD. These five SNPs were located from intron 2 of *SLC2A13* to 38.4 kb upstream of *LRRK2*. These SNPs were highly correlated with $r^2 > 0.83$ and were positioned within several LD blocks defined by the method of Gabriel *et al.*[16]. This is the first evidence that common variants proximal to *LRRK2* are associated with PD at genome-wide significance level.

Variants with the highest significance at the four loci detected in this study were common SNPs with risk allele frequencies of 0.50 (rs947211 on 1q32), 0.38 (rs4538475 on 4p15), 0.58 (rs11931074 on 4q22) and 0.08 (rs1994090 on 12q12) (**Table 1**). Population attributable risks for rs947211, rs4538475, rs11931074 and rs1994090 were estimated to be 13%, 8%, 18% and 3%, respectively.

Table 1 Summary of association results for representative SNPs that characterize the association of Parkinson's disease with 1q32 (*PARK16*), 4p15 (*BST1*), 4q22 (*SNCA*) and 12q12 (*LRRK2*)

				GWAS			Replication 1			GWAS + Replication 1		Replication 2			GWAS + Replication 1+2	
			Allele	MAF			MAF					MAF				
Locus	SNP	Pos (Mb)	Minor/ major	Case Ctrl	P_{trend}	OR (95% CI)	Case Ctrl	P_{trend}	OR (95% CI)	P_{cmh}	OR (95% CI)	Case Ctrl	P_{trend}	OR (95% CI)	P_{cmh}	OR (95% CI)
New PD loci																
1q32	rs16856139	203.91	T/C	0.10	2.55×10^{-6}	1.50	0.11	0.067	1.19	2.15×10^{-6}	1.35	0.10	0.015	1.42	1.02×10^{-7}	1.36
(*PARK16*)				0.14		(1.26–1.77)	0.13		(0.99–1.44)		(1.19–1.54)	0.13		(1.07–1.88)		(1.22–1.53)
	rs823128	203.98	G/A	0.10	2.09×10^{-5}	1.43	0.11	0.0056	1.31	4.67×10^{-7}	1.38	0.09	0.0028	1.53	4.88×10^{-9}	1.41
				0.14		(1.21–1.69)	0.13		(1.08–1.59)		(1.22–1.57)	0.14		(1.16–2.03)		(1.26–1.58)
	rs823122	203.99	C/T	0.10	7.98×10^{-5}	1.39	0.11	0.013	1.27	3.87×10^{-6}	1.34	0.09	0.0034	1.52	5.22×10^{-8}	1.37
				0.14		(1.18–1.64)	0.13		(1.05–1.54)		(1.18–1.52)	0.14		(1.15–2.01)		(1.22–1.54)
	rs947211	204.02	A/G	0.43	1.15×10^{-4}	1.23	0.42	1.35×10^{-6}	1.35	1.12×10^{-9}	1.28	0.42	2.80×10^{-4}	1.37	1.52×10^{-12}	1.30
				0.48		(1.11–1.37)	0.50		(1.19–1.52)		(1.18–1.38)	0.50		(1.16–1.63)		(1.21–1.39)
	rs823156	204.03	G/A	0.13	1.20×10^{-5}	1.40	0.14	0.012	1.25	6.45×10^{-7}	1.33	0.12	0.0013	1.52	3.60×10^{-9}	1.37
				0.17		(1.20–1.62)	0.17		(1.05–1.48)		(1.19–1.49)	0.17		(1.17–1.95)		(1.23–1.52)
	rs708730	204.04	G/A	0.14	2.60×10^{-5}	1.37	0.15	0.022	1.22	2.89×10^{-6}	1.30	0.12	0.0019	1.48	2.43×10^{-8}	1.33
				0.18		(1.18–1.59)	0.17		(1.03–1.44)		(1.17–1.46)	0.18		(1.15–1.89)		(1.21–1.48)
	rs11240572	204.07	A/C	0.13	1.66×10^{-4}	1.34	0.13	0.016	1.24	9.78×10^{-6}	1.30	0.12	0.0024	1.49	1.08×10^{-7}	1.33
				0.16		(1.15–1.56)	0.16		(1.04–1.48)		(1.16–1.46)	0.17		(1.15–1.92)		(1.20–1.48)
4p15	rs11931532	15.33	T/C	0.45	2.75×10^{-4}	1.22	0.47	1.86×10^{-4}	1.26	2.02×10^{-7}	1.23	0.47	0.0077	1.26	5.13×10^{-9}	1.24
(*BST1*)				0.40		(1.09–1.35)	0.42		(1.11–1.42)		(1.14–1.34)	0.41		(1.06–1.49)		(1.15–1.33)
	rs12645693	15.34	G/A	0.45	3.06×10^{-4}	1.21	0.47	3.00×10^{-4}	1.25	3.42×10^{-7}	1.23	0.47	0.0077	1.26	8.65×10^{-9}	1.24
				0.40		(1.09–1.35)	0.42		(1.11–1.41)		(1.14–1.33)	0.41		(1.06–1.49)		(1.15–1.33)
	rs4698412	15.35	A/G	0.38	5.28×10^{-5}	1.25	0.40	4.91×10^{-4}	1.24	1.03×10^{-7}	1.25	0.38	0.055	1.19	1.78×10^{-8}	1.24
				0.33		(1.12–1.40)	0.35		(1.10–1.40)		(1.15–1.35)	0.34		(1.00–1.42)		(1.15–1.33)
	rs4538475	15.35	A/G	0.41	4.05×10^{-5}	1.25	0.43	3.48×10^{-4}	1.25	5.98×10^{-8}	1.25	0.42	0.022	1.22	3.94×10^{-9}	1.24
				0.36		(1.12–1.40)	0.38		(1.10–1.41)		(1.15–1.35)	0.37		(1.03–1.46)		(1.16–1.34)
Loci located in or near autosomal dominant parkinsonism genes																
4q22	rs11931074	90.86	G/T	0.32	6.17×10^{-13}	1.50	0.36	2.12×10^{-5}	1.31	2.19×10^{-16}	1.41	0.38	0.034	1.21	7.35×10^{-17}	1.37
(*SNCA*)				0.42		(1.34–1.68)	0.42		(1.16–1.48)		(1.30–1.53)	0.43		(1.01–1.44)		(1.27–1.48)
	rs3857059	90.89	A/G	0.32	1.17×10^{-12}	1.49	0.36	6.92×10^{-5}	1.29	1.54×10^{-15}	1.40	0.38	0.041	1.20	5.68×10^{-16}	1.36
				0.41		(1.34–1.67)	0.42		(1.14–1.45)		(1.29–1.52)	0.43		(1.01–1.43)		(1.26–1.46)
	rs894278	90.95	G/T	0.43	7.68×10^{-5}	1.24	0.39	0.46	1.05	4.77×10^{-4}	1.15	0.42	0.020	1.22	3.28×10^{-5}	1.17
				0.38		(1.11–1.37)	0.38		(0.93–1.18)		(1.07–1.25)	0.37		(1.03–1.45)		(1.09–1.25)
	rs6532194	91.00	C/T	0.31	6.93×10^{-11}	1.44	0.36	0.0014	1.22	1.77×10^{-12}	1.35	0.37	0.040	1.21	4.15×10^{-13}	1.32
				0.40		(1.29–1.61)	0.41		(1.08–1.39)		(1.24–1.46)	0.41		(1.01–1.44)		(1.22–1.42)
12q12	rs1994090	38.71	G/T	0.11	4.45×10^{-5}	1.43	0.10	0.018	1.26	3.06×10^{-6}	1.36	0.12	0.0019	1.51	2.72×10^{-8}	1.39
(*LRRK2*)				0.08		(1.20–1.70)	0.08		(1.04–1.54)		(1.20–1.55)	0.08		(1.16–1.97)		(1.24–1.56)
	rs7304279	38.75	T/C	0.11	5.17×10^{-5}	1.42	0.10	0.026	1.25	5.10×10^{-6}	1.35	0.12	0.0022	1.50	5.06×10^{-8}	1.38
				0.08		(1.20–1.69)	0.08		(1.03–1.52)		(1.19–1.54)	0.09		(1.15–1.95)		(1.23–1.55)
	rs4768212	38.76	C/T	0.11	3.98×10^{-5}	1.43	0.10	0.057	1.21	1.10×10^{-5}	1.34	0.12	0.0020	1.51	1.09×10^{-7}	1.37
				0.08		(1.20–1.70)	0.08		(0.99–1.48)		(1.18–1.52)	0.08		(1.16–1.97)		(1.22–1.54)
	rs2708453	38.76	T/G	0.11	7.46×10^{-5}	1.41	0.10	0.063	1.21	2.04×10^{-5}	1.33	0.13	6.43×10^{-4}	1.57	9.67×10^{-8}	1.38
				0.08		(1.19–1.68)	0.08		(0.99–1.48)		(1.17–1.52)	0.08		(1.21–2.04)		(1.22–1.55)
	rs2046932	38.87	T/C	0.11	3.24×10^{-5}	1.44	0.10	0.039	1.23	5.47×10^{-6}	1.35	0.13	0.0017	1.52	4.34×10^{-8}	1.39
				0.08		(1.21–1.71)	0.08		(1.01–1.51)		(1.19–1.54)	0.09		(1.17–1.97)		(1.23–1.56)

Nucleotide positions refer to NCBI build 36. *P* values obtained in the case-control analysis using the Cochran-Armitage trend test (1 d.f.) are listed (P_{trend}). Combined *P* values (P_{cmh}) and combined ORs of the Cochran-Mantel-Haenzel test statistics are shown. MAF, minor allele frequency.

Next, we exchanged data with colleagues performing a GWAS of PD in individuals of European ancestry[17]. Their study found a strong association at the *MAPT* (microtubule-associated protein tau) region on 17q21. We genotyped our samples for six SNPs at the *MAPT* locus to evaluate these associations in the Asian population; however, the association with *MAPT* was not replicated in our study (**Supplementary Table 2** and **Supplementary Fig. 2**). Conversely, despite strong association signals in our scan of the samples from the Asian population, the association with *BST1* on 4p15 was not detected among individuals of European ancestry[17]. In contrast, the associations we found with *PARK16* and *LRRK2* were replicated among individuals of European ancestry[17]. These data provide evidence that *PARK16* and *LRRK2*, in addition to *SNCA*, are PD risk loci common to Asian- and European-descent populations and indicate that there is population genetic heterogeneity in the *MAPT* region and 4p15 (*BST1*) for PD susceptibility.

The *PARK16* region contains functionally interesting candidate genes for PD etiology. SLC41A1 is a magnesium (Mg^{2+}) transporter[18]. It is of interest that Mg^{2+} deficiency is thought to be an environmental risk factor for the amyotrophic lateral sclerosis

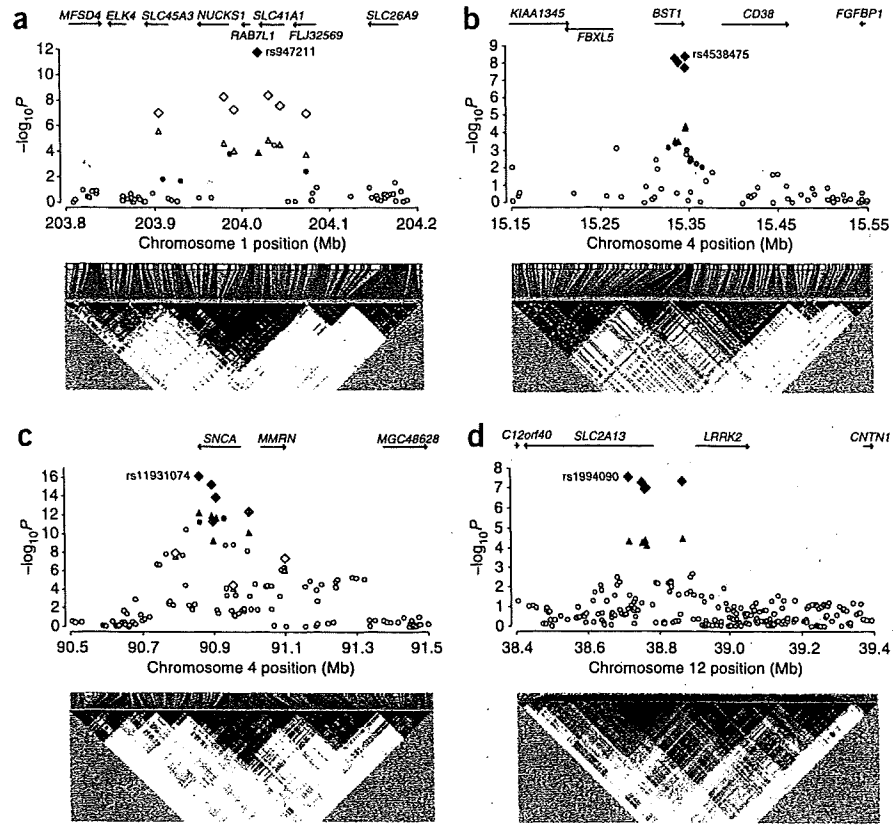

Figure 2 Regional association plots and linkage disequilibrium structure for the four PD risk loci. (**a**) 1q32 (*PARK16*). (**b**) 4p15 (*BST1*). (**c**) 4q22 (*SNCA*). (**d**) 12q12 (*LRRK2*). The $-\log_{10}$ *P* (Cochran-Armitage trend test) for association in the GWAS stage of SNPs across each region are shown as small triangles for SNPs that were selected for replication and as small circles for SNPs not selected. The $-\log_{10}$ combined *P* values (Cochran-Mantel-Haenszel test) for association in overall samples of SNPs selected for replication are shown as large diamonds. In each panel, the SNP with the most significant association in the combined analysis is listed. Proxies are indicated with colors determined from their pairwise r^2 from the JPT and CHB HapMap data (red, $r^2 > 0.8$; orange, $r^2 = 0.5$–0.8; yellow, $r^2 = 0.2$–0.5; white, $r^2 < 0.2$ or no information available). Positions are NCBI build 36 coordinates.

(ALS)-parkinsonism/dementia complex (MIM105500)[19]. Furthermore, RAB7L1 is a small GTP-binding protein that plays an important role in regulation of exo- and endocytotic pathways[20], and NUCKS1 is a nuclear protein containing several consensus phosphorylation sites for casein kinase II and cyclin-dependent kinases of unknown function[21]. We evaluated the relationships between the PD-associated SNPs and the transcript levels of genes in an available genome-wide gene expression database[22]. We found that rs947211 and ten tightly linked HapMap SNPs ($r^2 > 0.9$) were strongly associated with transcript levels of *NUCKS1* (rs947211, $P = 6.0 \times 10^{-15}$; rs823114, $P = 2.7 \times 10^{-34}$). These PD-susceptibility variants are the principal genetic determinants of variation in expression levels of *NUCKS1* (**Supplementary Fig. 3**). These data highlight *NUCKS1* as a promising candidate for association with PD that is worthy of additional follow-up.

The product of *BST1* on 4p15 catalyses formation of cyclic ADP-ribose (cADPR)[23]. cADPR mobilizes calcium (Ca^{2+}) from ryanodine-sensitive intracellular Ca^{2+} stores in the endoplasmic reticulum[24]. Disruption of Ca^{2+} homeostasis has recently been proposed as a possible cause of selective vulnerability of dopaminergic neurons in PD[25–27]. Associated SNPs in the *BST1* region may modify ADP-ribosylcyclase activity, thus leading to Ca^{2+} dyshomeostasis in dopaminergic neurons.

Two of the four susceptibility loci detected in our scan contained genes linked to autosomal dominant forms of parkinsonism. Gene overdosage is a potential mechanism for the influence of *SNCA* on PD because triplication and duplication of the *SNCA* locus has been seen in families with autosomal dominant parkinsonism[28]. SNPs with prominently low *P* values compared to other SNPs in the region were around the 3′ region of *SNCA*; these SNPs may function as enhancer or silencer elements, improve RNA stability or influence alternative splicing. The associated interval on 12q12 contains *SLC2A13* and the region upstream of *LRRK2*. Given prior evidence, *LRRK2* stands out as the most likely susceptibility gene for PD, although it remains possible that *SLC2A13*, which encodes a H^+-myoinositol cotransporter, may be the PD-related gene in this region[29]. Previous reports have investigated the association of SNPs in *LRRK2* with PD, but the results are a subject of dispute[30,31]. In the present study, it is noteworthy that the PD-associated intervals lie upstream of *LRRK2*. Increased kinase activity of mutant LRRK2 mediates neuronal toxicity[32,33]. PD-associated SNPs may play a role in transcriptional upregulation of *LRRK2*, leading to loss of dopaminergic neurons.

SNCA is a main component of Lewy bodies, a pathological hallmark of typical PD. The clinical features of individuals with *SNCA* duplication or *LRRK2* mutation similar to typical PD. 1.6% of sporadic PD cases among individuals of European ancestry have heterozygous *LRRK2* G2019S mutations[34]. These data support the close involvement of these genes with sporadic PD. Our data clearly show that the genes involved in autosomal dominant parkinsonism play a large part in the complex etiology of typical PD. Genes that cause autosomal dominant parkinsonism through their causative mutations also confer risk of typical PD through their common variants. Although further research is needed, this relationship between rare single-gene disorders and common multifactorial disorders may also be applicable for other disorders beyond PD.

Finally, *MAPT* mutations cause hereditary frontotemporal dementia and parkinsonism linked to chromosome 17 (FTDP-17), a type of autosomal dominant parkinsonism[35], and the *MAPT* H1 haplotype has been reported to be associated with several tauopathies[36–38]. Although the *MAPT* region is divided into two major haplotypes, H1 and H2, in Europeans, the H2 haplotype is absent in East Asians. Therefore, we believe that the differences observed between our study and the findings in populations of European descent reflect population differences in the genetic heterogeneity of PD etiology, although differences in allele frequencies and LD structure and a possible difference in the effect size between the European and East Asian populations may influence the detection power of the two scans.

Further increases in sample sizes for SNP-GWAS efforts and searches for copy number variation and rare variants will reveal additional genetic risk factors and further enhance our understanding of PD.

METHODS

Methods and any associated references are available in the online version of the paper at http://www.nature.com/naturegenetics/.

Note: Supplementary information is available on the Nature Genetics website.

ACKNOWLEDGMENTS

We are grateful to the individuals with PD who participated in this study. We also thank T. Takeshima and E. Ohta for PD samples, H. Inoko and K. Tokunaga for control samples, M. Kanagawa and K. Ura for editing, K. Yasuno and R. Ashida for analyses, and K. Yamada for genotyping. We appreciate all the volunteers and participating institutions of BioBank Japan for samples. This work was supported by a grant from Core Research for Evolutional Science and Technology (CREST), Japan Science and Technology Agency (JST); by the Global COE program and KAKENHI (17019044 and 19590990), both from the Ministry of Education, Culture, Sports, Science and Technology of Japan; and by the Grant-in-Aid for 'the Research Committee for the Neurodegenerative Diseases' of the Research on Measures for Intractable Diseases and Research Grant (H19-Genome-Ippan-001), all from the Ministry of Health, Labor and Welfare of Japan.

AUTHOR CONTRIBUTIONS

T. Toda conceived the study. W.S., I.M. and T. Toda designed the study. W.S., Y.N., C.I., M.K. and T.Y. performed genotyping. W.S. and T. Toda wrote the manuscript. W.S., T.K. and T. Tsunoda performed data analysis. W.S., I.M., Y.H., M.W., A.T., H.T., K.N., K.H., F.O., H.K., S.S., M.Y., N.H., M.M. and T. Toda managed Parkinson clinical information and DNA samples. M.K. and Y.N. managed DNA samples belonging to BioBank Japan. T. Toda obtained funding for the study.

Published online at http://www.nature.com/naturegenetics/.
Reprints and permissions information is available online at http://npg.nature.com/reprintsandpermissions/.

1. de Rijk, M.C. *et al.* Prevalence of parkinsonism and Parkinson's disease in Europe: the EUROPARKINSON collaborative study. *J. Neurol. Neurosurg. Psychiatry* **62**, 10–15 (1997).
2. Polymeropoulos, M.H. *et al.* Mutation in the α-synuclein gene identified in families with Parkinson's disease. *Science* **276**, 2045–2047 (1997).
3. Paisán-Ruíz, C. *et al.* Cloning of the gene containing mutations that cause *PARK8*-linked Parkinson's disease. *Neuron* **44**, 595–600 (2004).
4. Zimprich, A. *et al.* Mutations in *LRRK2* cause autosomal-dominant parkinsonism with pleomorphic pathology. *Neuron* **44**, 601–607 (2004).
5. Farrer, M.J. Genetics of Parkinson disease: paradigm shifts and future prospects. *Nat. Rev. Genet.* **7**, 306–318 (2006).
6. Thomas, B. & Beal, M.F. Parkinson's disease. *Hum. Mol. Genet.* **16 Spec No. 2**, R183–R194 (2007).
7. Warner, T.T. & Schapira, A.H. Genetic and environmental factors in the cause of Parkinson's disease. *Ann. Neurol.* **53**(Suppl 3), S16–S23 (2003).
8. Pals, P. *et al.* α-Synuclein promoter confers susceptibility to Parkinson's disease. *Ann. Neurol.* **56**, 591–595 (2004).
9. Mizuta, I. *et al.* Multiple candidate gene analysis identifies α-synuclein as a susceptibility gene for sporadic Parkinson's disease. *Hum. Mol. Genet.* **15**, 1151–1158 (2006).
10. Müller, J.C. *et al.* Multiple regions of α-synuclein are associated with Parkinson's disease. *Ann. Neurol.* **57**, 535–541 (2005).
11. Aharon-Peretz, J., Rosenbaum, H. & Gershoni-Baruch, R. Mutations in the glucocerebrosidase gene and Parkinson's disease in Ashkenazi Jews. *N. Engl. J. Med.* **351**, 1972–1977 (2004).
12. Maraganore, D.M. *et al.* High-resolution whole-genome association study of Parkinson disease. *Am. J. Hum. Genet.* **77**, 685–693 (2005).
13. Fung, H.C. *et al.* Genome-wide genotyping in Parkinson's disease and neurologically normal controls: first stage analysis and public release of data. *Lancet Neurol.* **5**, 911–916 (2006).
14. Pankratz, N. *et al.* Genomewide association study for susceptibility genes contributing to familial Parkinson disease. *Hum. Genet.* **124**, 593–605 (2009).
15. Welcome Trust Case Control Consortium. Genome-wide association study of 14,000 cases of seven common diseases and 3,000 shared controls. *Nature* **447**, 661–678 (2007).
16. Gabriel, S.B. *et al.* The structure of haplotype blocks in the human genome. *Science* **296**, 2225–2229 (2002).
17. Simón-Sánchez, J. *et al.* Genome-wide association study reveals genetic risk underlying Parkinson's disease. *Nat. Genet.* advance online publication, doi:10.1038/ng.487 (15 November 2009).
18. Kolisek, M. *et al.* SLC41A1 is a novel mammalian Mg^{2+} carrier. *J. Biol. Chem.* **283**, 16235–16247 (2008).
19. Garruto, R.M. *et al.* Disappearance of high-incidence amyotrophic lateral sclerosis and parkinsonism-dementia on Guam. *Neurology* **35**, 193–198 (1985).
20. Shimizu, F. *et al.* Cloning and chromosome assignment to 1q32 of a human cDNA (*RAB7L1*) encoding a small GTP-binding protein, a member of the RAS superfamily. *Cytogenet. Cell Genet.* **77**, 261–263 (1997).
21. Ostvold, A.C. *et al.* Molecular cloning of a mammalian nuclear phosphoprotein NUCKS, which serves as a substrate for Cdk1 *in vivo*. *Eur. J. Biochem.* **268**, 2430–2440 (2001).
22. Dixon, A.L. *et al.* A genome-wide association study of global gene expression. *Nat. Genet.* **39**, 1202–1207 (2007).
23. Yamamoto-Katayama, S. *et al.* Crystallographic studies on human BST-1/CD157 with ADP-ribosyl cyclase and NAD glycohydrolase activities. *J. Mol. Biol.* **316**, 711–723 (2002).
24. Lee, H.C. *et al.* Physiological functions of cyclic ADP-ribose and NAADP as calcium messengers. *Annu. Rev. Pharmacol. Toxicol.* **41**, 317–345 (2001).
25. Wilson, C.J. & Callaway, J.C. Coupled oscillator model of the dopaminergic neuron of the substantia nigra. *J. Neurophysiol.* **83**, 3084–3100 (2000).
26. Chan, C.S. *et al.* 'Rejuvenation' protects neurons in mouse models of Parkinson's disease. *Nature* **447**, 1081–1086 (2007).
27. Surmeier, D.J. Calcium, ageing, and neuronal vulnerability in Parkinson's disease. *Lancet Neurol.* **6**, 933–938 (2007).
28. Singleton, A.B. *et al.* α-Synuclein locus triplication causes Parkinson's disease. *Science* **302**, 841 (2003).
29. Uldry, M. *et al.* Identification of a mammalian H(+)-myo-inositol symporter expressed predominantly in the brain. *EMBO J.* **20**, 4467–4477 (2001).
30. Skipper, L. *et al.* Comprehensive evaluation of common genetic variation within *LRRK2* reveals evidence for association with sporadic Parkinson's disease. *Hum. Mol. Genet.* **14**, 3549–3556 (2005).
31. Biskup, S. *et al.* Common variants of *LRRK2* are not associated with sporadic Parkinson's disease. *Ann. Neurol.* **58**, 905–908 (2005).
32. Smith, W.W. *et al.* Kinase activity of mutant LRRK2 mediates neuronal toxicity. *Nat. Neurosci.* **9**, 1231–1233 (2006).
33. West, A.B. *et al.* Parkinson's disease-associated mutations in leucine-rich repeat kinase 2 augment kinase activity. *Proc. Natl. Acad. Sci. USA* **102**, 16842–16847 (2005).
34. Gilks, W.P. *et al.* A common *LRRK2* mutation in idiopathic Parkinson's disease. *Lancet* **365**, 415–416 (2005).
35. Hutton, M. *et al.* Association of missense and 5′-splice-site mutations in tau with the inherited dementia FTDP-17. *Nature* **393**, 702–705 (1998).
36. Pittman, A.M. *et al.* Linkage disequilibrium fine mapping and haplotype association analysis of the tau gene in progressive supranuclear palsy and corticobasal degeneration. *J. Med. Genet.* **42**, 837–846 (2005).
37. Webb, A. *et al.* Role of the tau gene region chromosome inversion in progressive supranuclear palsy, corticobasal degeneration, and related disorders. *Arch. Neurol.* **65**, 1473–1478 (2008).
38. Healy, D.G. *et al.* Tau gene and Parkinson's disease: a case-control study and meta-analysis. *J. Neurol. Neurosurg. Psychiatry* **75**, 962–965 (2004).

FEBS Letters 584 (2010) 1073–1079

ELSEVIER

FEBS Letters

journal homepage: www.FEBSLetters.org

PINK1 is recruited to mitochondria with parkin and associates with LC3 in mitophagy

Sumihiro Kawajiri [a,1], Shinji Saiki [a,1], Shigeto Sato [a], Fumiaki Sato [b], Taku Hatano [a], Hiroto Eguchi [a], Nobutaka Hattori [a,*]

[a] Department of Neurology, Juntendo University School of Medicine, 2-1-1 Hongo, Bunkyo-ku, Tokyo 113-8421, Japan
[b] Research Institute for Disease of Old Age, Juntendo University School of Medicine, 2-1-1 Hongo, Bunkyo-ku, Tokyo 113-8421, Japan

ARTICLE INFO

Article history:
Received 16 December 2009
Revised 29 January 2010
Accepted 2 February 2010
Available online 12 February 2010

Edited by Jesus Avila

Keywords:
PTEN-induced putative kinase 1
Parkin
Mitophagy
Autophagy
Parkinson's disease

ABSTRACT

Mutations in *PTEN-induced putative kinase 1 (PINK1)* cause recessive form of Parkinson's disease (PD). PINK1 acts upstream of parkin, regulating mitochondrial integrity and functions. Here, we show that PINK1 in combination with parkin results in the perinuclear mitochondrial aggregation followed by their elimination. This elimination is reduced in cells expressing PINK1 mutants with wild-type parkin. Although wild-type PINK1 localizes in aggregated mitochondria, PINK1 mutants localization remains diffuse and mitochondrial elimination is not observed. This phenomenon is not observed in autophagy-deficient cells. These results suggest that mitophagy controlled by the PINK1/parkin pathway might be associated with PD pathogenesis.

Structured summary:
MINT-7557195: *PINK1* (uniprotkb:Q9BXM7) *physically interacts* (MI:0915) with *LC3* (uniprotkb:Q9GZQ8) by *anti tag coimmunoprecipitation* (MI:0007)
MINT-7557109: *LC3* (uniprotkb:Q9GZQ8) and *PINK1* (uniprotkb:Q9BXM7) *colocalize* (MI:0403) by *fluorescence microscopy* (MI:0416)
MINT-7557121: *tom20* (uniprotkb:Q15388) and *PINK1* (uniprotkb:Q9BXM7) *colocalize* (MI:0403) by *fluorescence microscopy* (MI:0416)
MINT-7557138: *parkin* (uniprotkb:O60260), *PINK1* (uniprotkb:Q9BXM7) and *tom20* (uniprotkb:Q15388) *colocalize* (MI:0403) by *fluorescence microscopy* (MI:0416)
MINT-7557173: *LC3* (uniprotkb:Q9GZQ8) *physically interacts* (MI:0915) with *PINK1* (uniprotkb:Q9BXM7) by *anti bait coimmunoprecipitation* (MI:0006)

1. Introduction

Parkinson's disease (PD) is a neurodegenerative disease characterized by loss of dopaminergic neurons in the substantia nigra. Mitochondrial dysfunction has been proposed as a major factor in the pathogenesis of sporadic and familial PD [1. In particular, the identification of mutations in *PTEN-induced putative kinase 1 (PINK1)* has strongly implicated mitochondrial dysfunction in the pathogenesis of PD [2]. PINK1 contains an N-terminal mitochondrial targeting sequence (MTS) and a serine/threonine kinase domain [2].

Several studies have shown that PINK1 acts upstream of parkin in the same genetic pathway [3,4]. Overexpression of PINK1 promotes mitochondrial fission [5]. Fission followed by selective fusion segregates dysfunctional mitochondria and permits their removal by autophagy [6]. Parkin is associated with mitochondrial elimination in cultured cells treated with the mitochondrial uncoupler carbonyl cyanide *m*-chlorophenylhydrazone (CCCP) [7], but little is known about the biological function of PINK1 in this context. Likewise, although co-overexpressed both PINK1 and parkin colocalized with mitochondria [8] and are associated with mitochondrial autophagy (mitophagy) [9], the exact mechanism of the mitochondrial elimination via autophagy has not been examined.

Here, we describe the characterization of mitophagy induced by co-overexpressing both proteins and report that the phenomenon is dependent on PINK1 kinase activity and mitochondrial localization.

Abbreviations: CCCP, carbonyl cyanide *m*-chlorophenylhydrazone; 3-MA, 3-methyladenine; MEFs, mouse embryonic fibroblasts; MTS, mitochondrial targeting sequence; PD, Parkinson's disease; PINK1, PTEN-induced putative kinase 1; UPS, ubiquitin–proteasome system

* Corresponding author. Address: Department of Neurology, Juntendo University School of Medicine, 2-1-1 Hongo, Bunkyo-ku, Tokyo, 113-8421, Japan. Fax: +81 3 5800 0547.
E-mail address: nhattori@juntendo.ac.jp (N. Hattori).
[1] Joint first authors.

0014-5793/$36.00
doi:10.1016/j.febslet.2010.02.016

Furthermore, we found that PINK1 interacts with LC3–phospholipid conjugate (LC3-II), a well established marker for autophagosomes [10]. These results provide novel insights into the pathogenesis of PD.

2. Materials and methods

2.1. Antibodies

Anti-FLAG antibodies (M2, polyclonal) and anti-LC3B antibody (rabbit) were obtained from Sigma. Anti-actin antibody (mouse) was from Millipore. Anti-Tom20 antibody (rabbit) was from Santa Cruz Biotechnology. Anti-LDH antibody (goat) was from Abcam. Anti-LC3 antibody (rabbit) was from MBL. Secondary antibodies, conjugated to horseradish peroxidase, were from GE HealthCare Bio-Sciences and Alexa Fluor 488, 546, 594, and 647 conjugated secondary antibodies were from Invitrogen-Molecular Probes.

2.2. Plasmids

A cDNA encoding wild-type PINK1 was amplified with appropriate primers and ligated into the BamHI sites of the (C-terminal tagged) 3xFLAG pCMV-10™ expression plasmid (Sigma). Mutations in PINK1 were introduced by site-directed mutagenesis (Stratagene) according to manufacturer's instructions. GFP-parkin was subcloned into pcDNA3.1 (Invitrogen).

2.3. Cell culture

HeLa, HEK293 cells and Atg7$^{+/+}$ and $^{-/-}$ mouse embryonic fibroblasts (MEFs) (a gift from Dr. Komatsu) were grown in DMEM (Sigma) supplemented with 10% FBS (Sigma) and 1% penicillin–streptomycin (Invitrogen) at 37 °C and 5% CO_2. For pharmacological studies, E64d, pepstatin A, rapamycin, 3-MA, and CCCP (Sigma) were added at indicated times and concentrations.

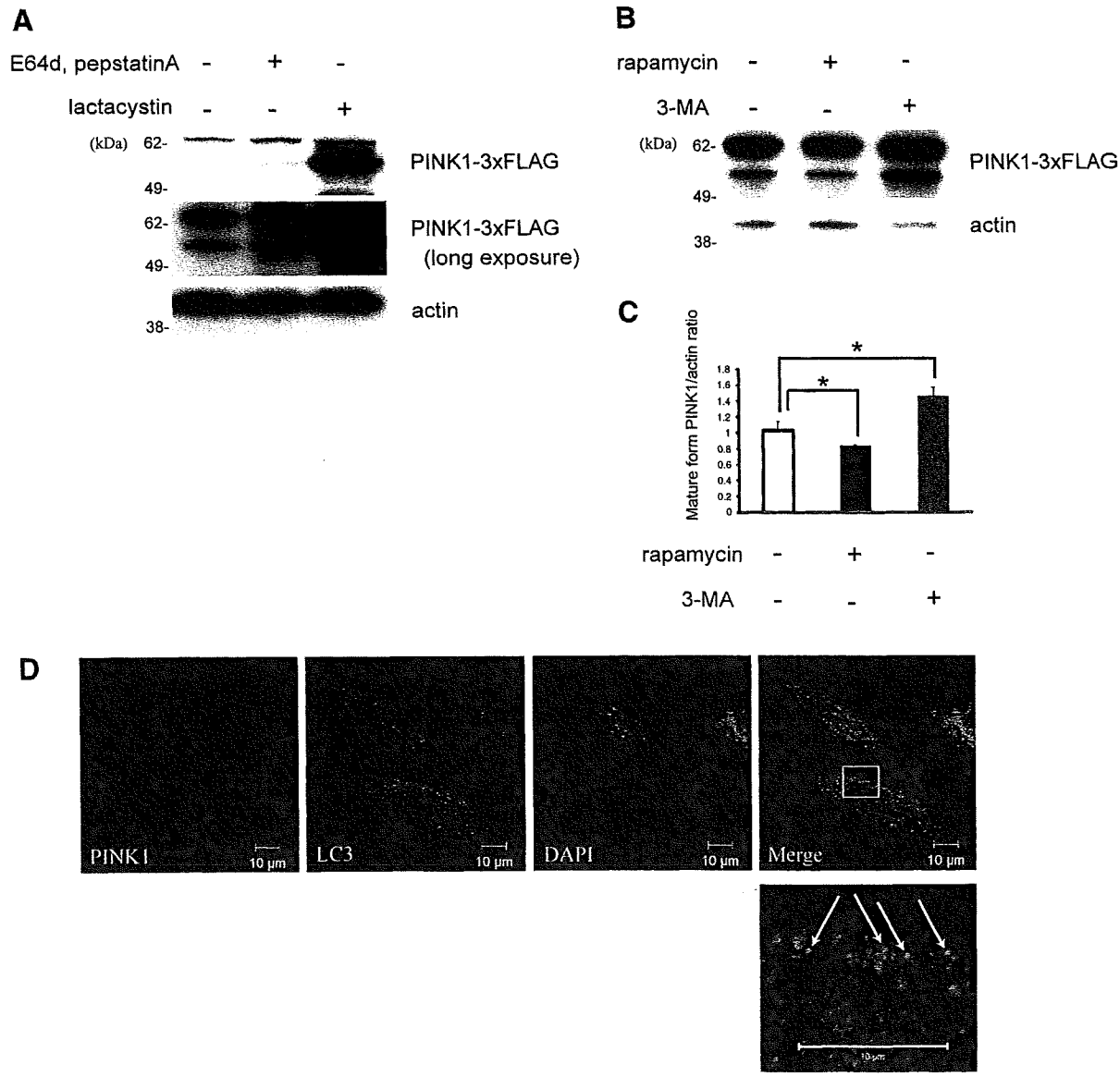

Fig. 1. PINK1 is degraded by autophagy as well as by the ubiquitin–proteasome system. (A and B) PINK1 levels in HEK293 cells stably expressing PINK1-3xFLAG treated or untreated with E64d (10 μg/ml) + pepstatin A (10 μg/ml) or lactacystin (10 μM) (A), and 3-MA (10 mM) or rapamycin (200 nM) (B), for 24 h were analyzed by immunoblotting with anti-FLAG antibodies (M2). The bottom panels show actin as loading control. (C) Quantification of (B); *$P < 0.05$. Error bars indicate standard deviation of at least three experiments. (D) Immunocytochemistry of HeLa cells transiently overexpressing PINK1-3xFLAG, 24 h after transfection. PINK1 or LC3 are in red or green, respectively. The boxed area is shown in the bottom image at a higher magnification. Bars, 10 μM.

2.4. Cell transfection and establishment of stable cell lines

Cells were transfected with the indicated plasmids using Lipofectamine 2000 (Invitrogen) and Lipofectamine LTX with PLUS Reagent (Invitrogen) according to manufacturer's instructions. For stable overexpression of PINK1, HEK293 cells were transfected with PINK1 plasmids and then selected using G418.

2.5. Immunocytochemistry

Cells were fixed with 4% paraformaldehyde, permeabilized with 1× PBS containing 0.5% Triton X-100, and incubated in PBS containing 10% FBS and 1% BSA. Cells were then incubated overnight with primary antibodies, followed by incubation with secondary antibodies for 1 h. Cells were then mounted with Vectashield containing DAPI (Vector Laboratories). Cells were visualized using a ZEISS LSM510 confocal microscope.

2.6. Cell fractionation

Cells were fractionated using the mitochondrial isolation kit for cultured cells (Pierce) according to manufacturer's instructions.

2.7. Immunoprecipitation and immunoblotting

Cells were lysed on ice in lysis buffer [10 mM Tris–HCl (pH 7.5), 150 mM NaCl, 1 mM EDTA, 1% NP-40, and protease inhibitors (complete, Mini, EDTA-free, (Roche Applied Science))]. Cell lysates were immunoprecipitated using Dynabeads protein G (Invitrogen) according to manufacturer's instructions and immunoblotting was performed previously described elsewhere [11].

3. Results and discussion

3.1. PINK1 is degraded by autophagy as well as by the ubiquitin–proteasome system (UPS)

Previous studies have shown that PINK1 is degraded by the UPS [12], but it remains unclear whether autophagy also affects its degradation. We, therefore, tested whether PINK1 could be degraded via the UPS and/or autophagy, using HEK293 cells stably expressing PINK1-3xFLAG. Immunoblot analysis identifies PINK1 in two bands. The upper band represents full-length PINK1 (~66 kDa), whereas the lower band represents the mature form of PINK1 (~55 kDa), in which the MTS has been removed [13,14]. As others

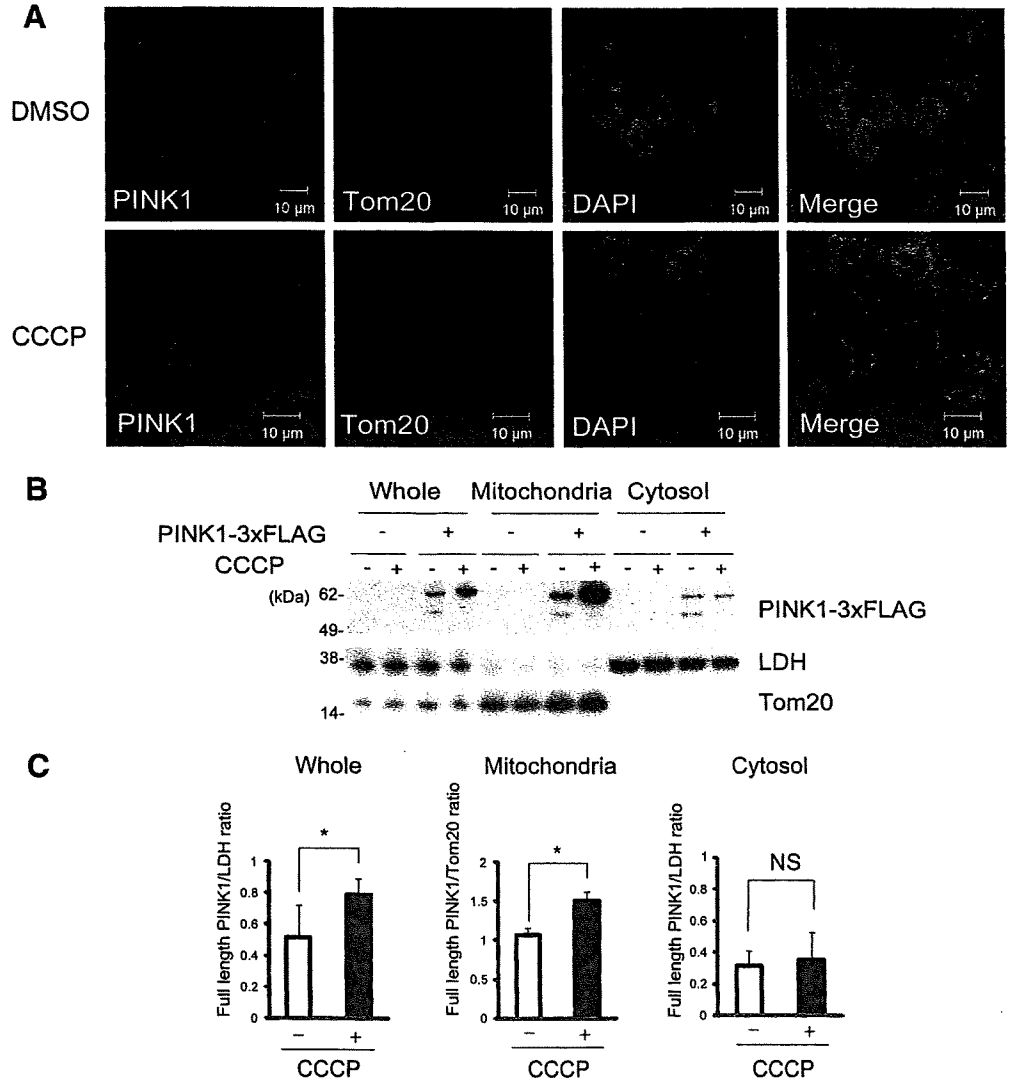

Fig. 2. PINK1 is recruited to depolarized mitochondria. (A) Immunocytochemistry of HEK293 cells stably expressing PINK1-3xFLAG treated with DMSO or CCCP (10 μM) for 3 h. PINK1 or Tom20 are in green or red, respectively. Bars, 10 μM. (B) HEK293 cells stably expressing 3xFLAG-empty vector or PINK1-3xFLAG treated with DMSO or CCCP (10 μM) for 3 h were fractionated and immunoblotted for FLAG, Tom20, and LDH. (C) Quantification of (B); *$P < 0.05$. NS, non-significant. Error bars indicate standard deviation of at least three experiments.

have shown [12], levels of mature form PINK1 were increased by treatment with a proteasome inhibitor (lactacystin) (Fig. 1A). Also, they were increased by lysosome protease inhibitors (E64d + pepstatin A), which block autophagic flux (Fig. 1A). Next, we investigated the effects of other autophagy modulators (rapamycin and 3-methyladenine (3-MA)) on levels of PINK1. As expected, rapamycin treatment decreased mature form PINK1 levels, although 3-MA treatment increased them (Fig. 1B and C). Immunocytochemistry of HeLa cells transiently overexpressing PINK1-3xFLAG demonstrated partial colocalization of PINK1 with endogenous LC3 (an autophagosomal marker) (Fig. 1D). These data suggested that PINK1 is degraded via autophagy as well as by the UPS.

3.2. PINK1 is recruited to depolarized mitochondria

In cultured cells treated with CCCP, parkin is selectively recruited to degraded mitochondria and promotes mitophagy [7]. PINK1 and parkin function in the same genetic pathway to regulate mitochondrial integrity [3,4]. To investigate the interaction between depolarized mitochondria and PINK1, we tested for a change of PINK1 localization following treatment with CCCP. In HEK293 cells stably expressing PINK1, mitochondria stained with antibody against Tom20, a receptor protein of the mitochondrial outer membrane, were aggregated around the nucleus and fragmented and showed marked accumulation of PINK1 (Fig. 2A). The mitochondrial translocation of PINK1, caused by CCCP, was also assayed by immunoblotting. Levels of full-length PINK1 in the mitochondrial fraction were increased by CCCP treatment (Fig. 2B and C).

3.3. Mitochondrial elimination is accomplished by overexpression of wild-type PINK1 in combination with parkin

PINK1 has been reported to promote parkin translocation to mitochondria [8]. To further investigate the molecular interaction between PINK1 and parkin, the following experiments with HeLa cells overexpressing both PINK1 and parkin were performed. Twenty-four hours after transfection, mitochondrial aggregation and recruitment of PINK1 and parkin to the aggregated mitochondria were observed only in cells positive for GFP-parkin and PINK1-3xFLAG. Moreover, parkin completely colocalized with aggregated mitochondria (Fig. 3A and B). Partial colocalization of wild-type PINK1 with parkin has been previously reported in cells overexpressing both PINK1 and parkin; however, the association with mitochondria was not examined [15]. Also, parkin colocalization with PINK1 in aggregated mitochondria has been previously reported [8]. To confirm the exact effect of both PINK1 and parkin on mitochondria, we examined the fate of the degraded mitochondria, 48 h after transfection. In cells overexpressing both PINK1 and parkin, the mitochondria were completely absent, while mitochondria were still present in cells overexpressing either PINK1 or parkin (Fig. 3C). These data indicate that both PINK1 and parkin might be indispensable for mitochondrial elimination.

3.4. PINK1 mutants remain diffusely distributed and are not recruited to mitochondria, resulting in reduced mitochondrial elimination

PD-associated mutations in PINK1 have been found in both the kinase and C-terminal domains [2,16]. Among these mutations, G309D, L347P, and G409V are expected to cause a reduction in the kinase activity of PINK1 [13,14,17]. Therefore, we generated PINK1 mutants with G309D, L347P and G409V and two deletion mutants without the MTS (ΔN: deleted amino acids 156–581 and KD: deleted amino acids 156–509) and performed similar transfection experiments to those described above. Neither recruitment of parkin and/or mutant PINK1 to the mitochondria nor mitochondrial aggregation was detected 24 h after transfection (data not shown). Forty-eight hours after transfection, the G309D/L347P/G409V mutants preserved their mitochondrial localization, whilst less mitochondrial elimination was detected compared with those cells expressing both wild-type PINK1 and parkin. The ΔN/KD mutants were diffusely distributed without apparent colocalization to the mitochondria and no mitochondrial elimination was observed (Fig. 4A–C). Also, we confirmed mitochondrial elimination by immunoblotting. Levels of Tom20 were decreased in cells expressing both parkin and wild-type PINK1 but not in the cells expressing PINK1 mutants (Fig. 4D and E). These findings suggested that the

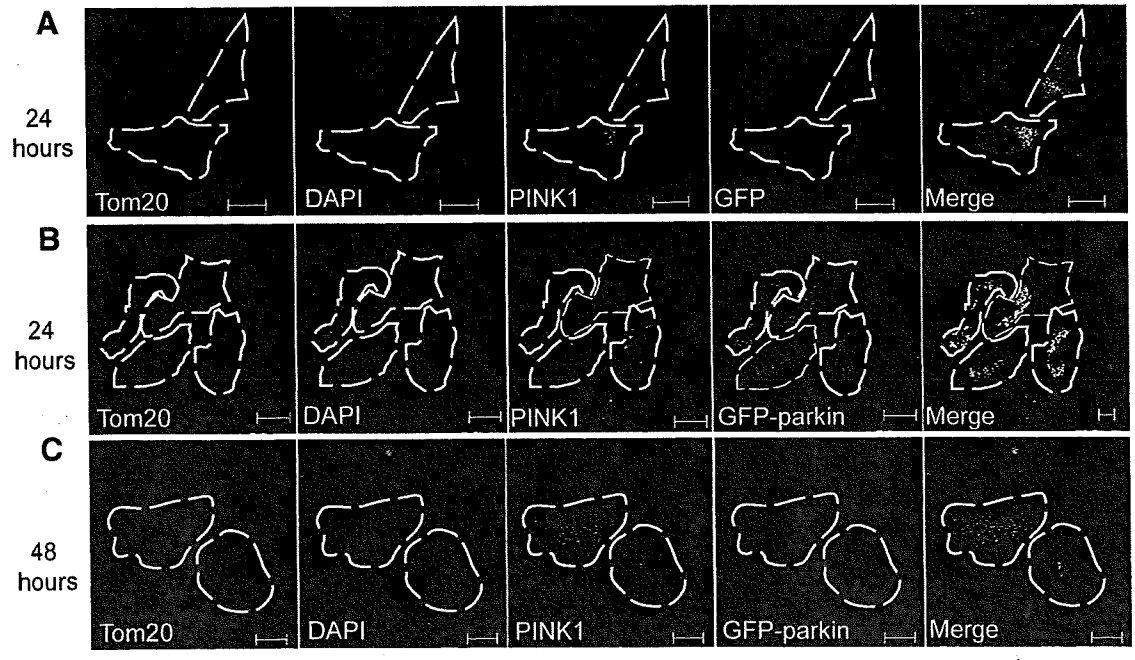

Fig. 3. Mitochondrial elimination is accomplished by overexpression of wild-type PINK1 in combination with parkin. (A and B) Immunocytochemistry of HeLa cells 24 h after transient co-overexpression of wild-type PINK1-3xFLAG (PINK1-WT) and GFP-empty vector (GFP) (A) or GFP-parkin (B) and 48 h after transient co-overexpression of PINK1-WT and GFP-parkin (C). Tom20, wild-type PINK1, or GFP are red, white, or green, respectively. Bars, 10 μm.

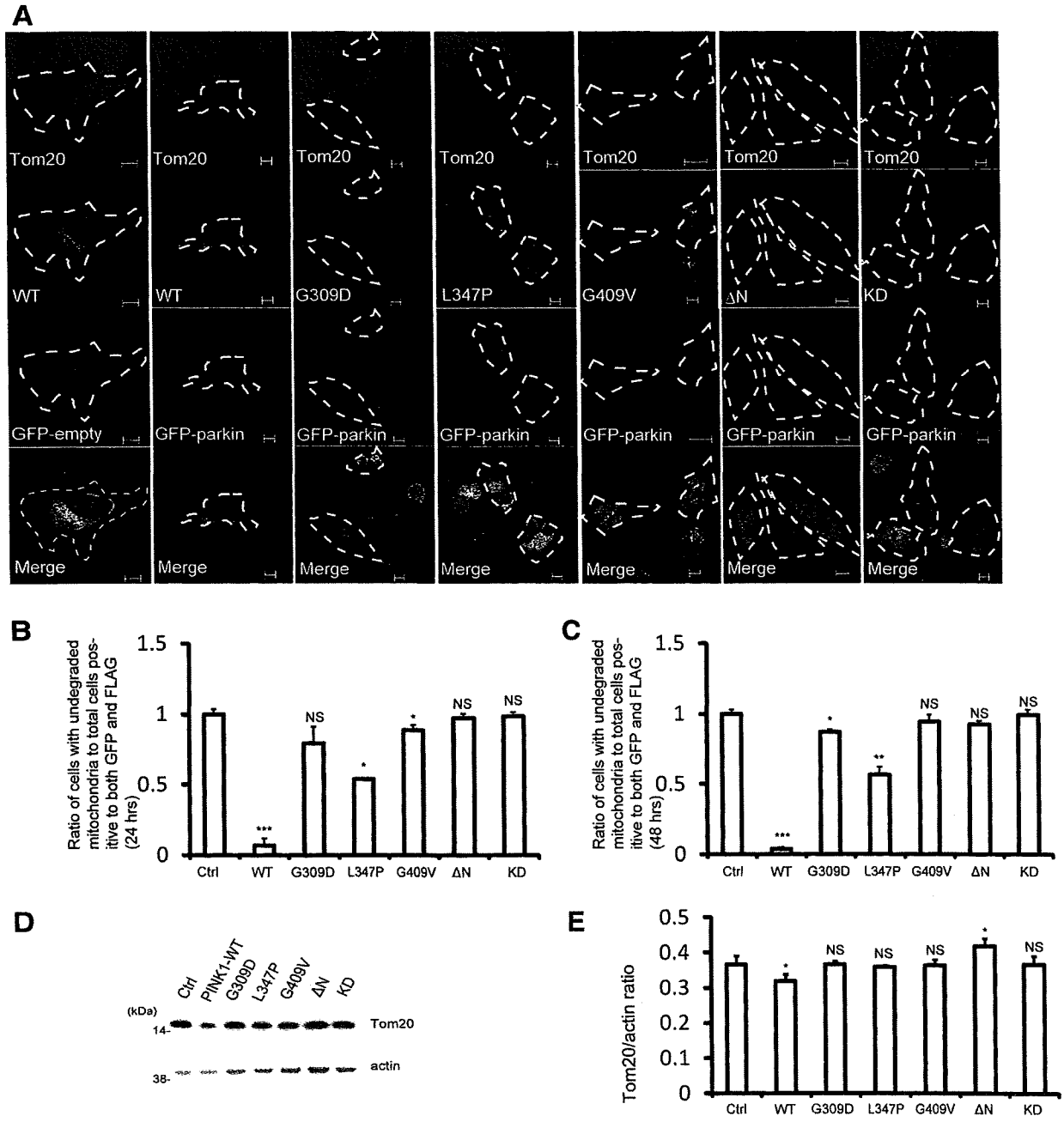

Fig. 4. PINK1 mutants remain diffusely distributed and are not recruited to mitochondria, resulting in reduced mitochondrial elimination. (A) Immunocytochemistry of HeLa cells transiently overexpressing GFP-empty vector and PINK1-3xFLAG (WT) as control, and GFP-parkin and PINK1-3xFLAG (WT or various mutants), 48 h after transfection. Tom20, WT and PINK1 mutants, or GFP are in red, white, or green, respectively. Bars, 10 μm. (B and C) Ratio of cells with undegraded mitochondria to total cells positive for both GFP and FLAG, 24 h (B) and 48 h (C) after transfection are shown in the graph. (D) Levels of Tom20 in HeLa cells transiently overexpressing GFP-empty vector and PINK1-3xFLAG (WT), and GFP-parkin and PINK1-3xFLAG (WT or various mutants) were analyzed with immunoblotting. (E) Quantification of (D); error bars indicate standard deviation of at least three experiments. $^{*}P < 0.05$, $^{**}P < 0.01$, $^{***}P < 0.001$. NS, non-significant.

kinase activity and mitochondrial localization of PINK1 are indispensable for mitochondrial elimination.

3.5. Overexpression of wild-type PINK1 in combination with parkin induces mitophagy

Very recently, it has been reported aggregated mitochondria in cells overexpressing both PINK1 and parkin colocalize with lysosomes as well as autophagosomes [9]. However, the fate of perinuclear aggregated mitochondria has not been examined. Therefore, we checked whether PINK1–parkin dependent mitochondrial elimination was dependent on mitophagy. Mitochondrial elimination was enhanced by overexpression of PINK1 with parkin in wild-type MEFs. On the other hand, Atg7$^{-/-}$ MEFs, which lack a key component of the autophagy system, retain expression of Tom20 (Fig. 5A and B). To further analyze this hypothesis, we examined the change of endogenous LC3 distribution following both PINK1 and parkin overexpression. We confirmed accumulation of parkin, which overlaps with aggregated mitochondria (refer to Fig. 3), in cells expressing both wild-type proteins. Likewise, endogenous LC3 mainly colocalized with wild-type PINK1, adjoined to the outer mitochondrial membrane, but did not colocalize with G409V or ΔN

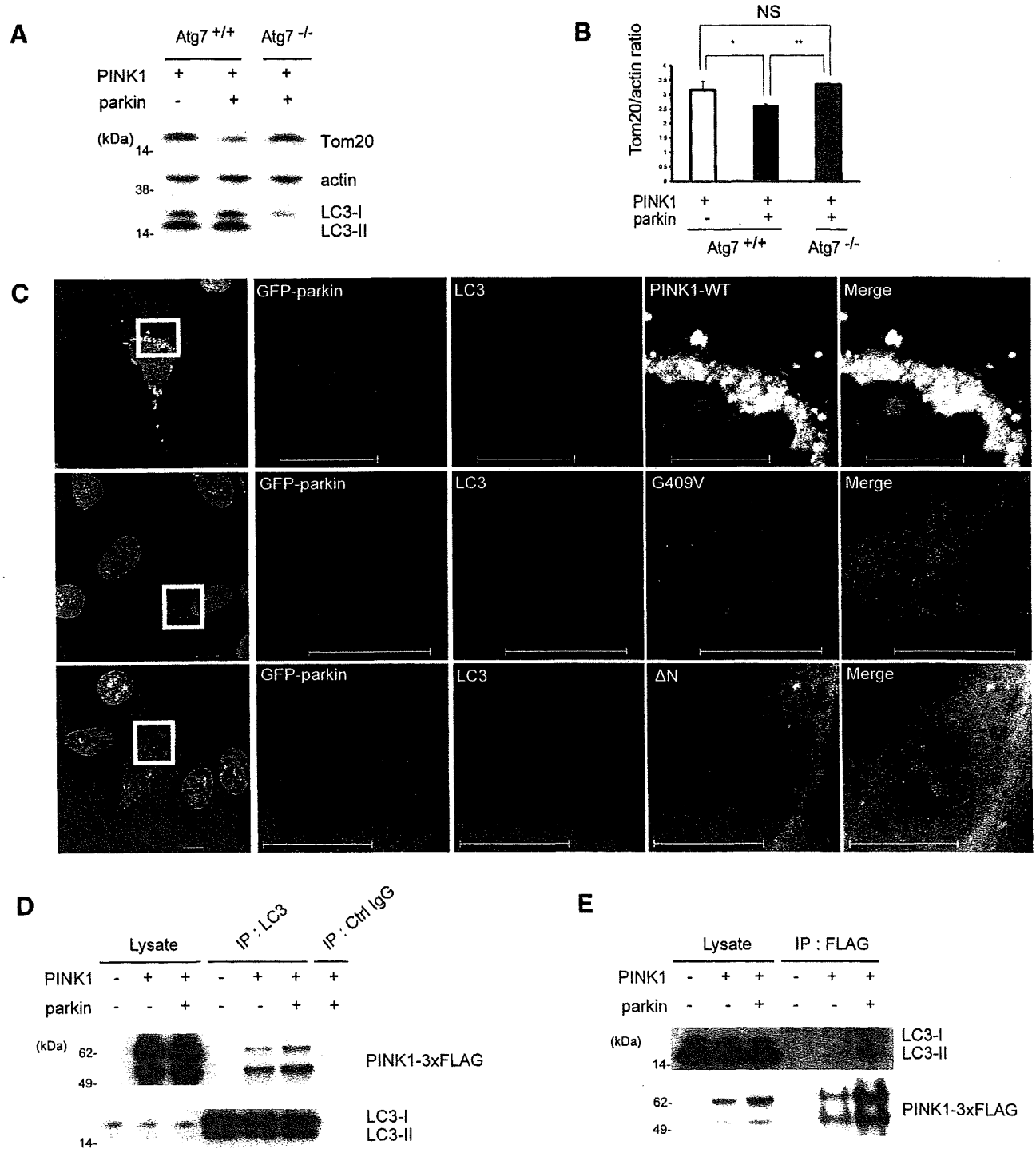

Fig. 5. Overexpression of wild-type PINK1 in combination with parkin induces mitophagy. (A) Levels of Tom20 in Atg7$^{+/+}$ MEFs overexpressing GFP-empty vector and PINK1-3xFLAG and those in Atg7$^{+/+}$ and Atg7$^{-/-}$ MEFs overexpressing GFP-parkin and PINK1-3xFLAG, 48 h after transfection were analyzed by immunoblotting. (B) Quantification of (A); error bars indicate standard deviation of at least three experiments. $^{*}P < 0.05$, $^{**}P < 0.01$, NS, non-significant. (C) Immunocytochemistry of HeLa cells transiently overexpressing GFP-parkin and PINK1-3xFLAG (wild-type, G409V, and ΔN), 24 h after transfection. PINK1 (WT and mutants), LC3, or GFP-parkin are in white, red, or green, respectively. The boxed areas are shown in the three right-hand images at a higher magnification. Bars, 10 μm. (D and E) HeLa cells overexpressing 3xFLAG-empty vector and GFP-empty vector, PINK1-3xFLAG and GFP-empty vector, or PINK1-3xFLAG and GFP-parkin, 24 h after transfection were immunoprecipitated with anti-LC3 antibodies (D) or anti-FLAG antibodies (E) and immunoblotted for FLAG or LC3. Immunoblotting of total lysates was performed to test the expression levels. IP, immunoprecipitation.

(Fig. 5C), nor with G309D, L347P and KD (data not shown). LC3 also partially colocalized with parkin. Compared with Fig. 1D, the colocalization of endogenous LC3 with PINK1 was markedly enhanced. Next, to investigate direct interaction, cell lysates were immunoprecipitated using anti-LC3 antibodies and immunoblotted with anti-FLAG antibodies (Fig. 5D). The reverse immunoprecipitation was also performed (Fig. 5E). These results allowed us to conclude that PINK1 binds with LC3-II. Taken together, we concluded that mitochondrial elimination by the PINK1–parkin pathway is dependent on mitochondrial autophagic activity.

In this study, we have found that overexpression of both proteins enhances mitochondrial elimination via autophagy. In

contrast to the results of a *Drosophila* study, a PINK1–parkin pathway promotes mitochondrial enlargement or aggregation in mammalian cellular models [8,18]. However, only PINK1 overexpressing cells exhibit longer mitochondria with increased interconnectivity, but the abnormal mitochondria do not elicit an autophagic response [12]. Consistent with this, wild-type PINK1 overexpression did not change the level of endogenous LC3-II (data not shown). Therefore, coordinating activation of parkin and PINK1 contributes to mitophagy.

PINK1 localization in mitochondria is dependent on its MTS region and it exhibits autophosphorylation activity in vitro [2,13,14]. Parkin is recognized as an in vivo substrate of PINK1 and parkin site-direct phosphorylation by wild-type PINK1 is critical for the translocation of parkin into the mitochondria in cellular and *Drosophila* models [8]. In agreement with this report, our study showed that parkin recruitment to the mitochondria by PINK1 was dependent on PINK1 kinase activity.

Silencing of PINK1 with shRNA increased mitochondrial fission and induced mitophagy [12]. Although PINK1 overexpression is protective against oxidative stress-induced apoptotic cell death [2,19,20], excess wild-type PINK1 without parkin overexpression does not elicit mitochondrial autophagy [12]. Our immunocytochemical experiments revealed that PINK1 co-overexpressed with parkin colocalized mainly with LC3-positive vesicles and partially with perinuclear aggregated mitochondria, which were expected to colocalize with aggregated parkin. In addition, molecular binding between PINK1 and LC3-II was confirmed by immunoprecipitation, which suggests that association between PINK1 and LC3 contribute to mitophagy. Combined with the observation by Vives-Bausa et al., although it is not clear whether an excess of mitophagy would be harmful to cells, a PINK1–parkin pathway, which is regulated by kinase activity and/or the mitochondrial localization of PINK1, would control mitochondrial maintenance via the autophagic machinery.

Acknowledgments

We thank Drs. Masaaki Komatsu and Yu-shin Sou (Laboratory of Frontier Science, Tokyo Metropolitan Institute of Medical Science) for providing Atg7$^{-/-}$ MEFs and Hattori's laboratory members for helpful discussions. We are grateful to Drs. Junichi Nakamoto, Yoko Imamichi, and Akiko Egashira for technical assistance. This study was supported by a Young Scientist Grant (F.S. and S. Saiki), an All Japan Coffee Association Grant (S. Saiki), a Takeda Scientific Association Grant (S. Saiki) and a Grant from Nagao Memorial Fund (S. Saiki).

References

[1] Abou-Sleiman, P.M., Muqit, M.M. and Wood, N.W. (2006) Expanding insights of mitochondrial dysfunction in Parkinson's disease. Nat. Rev. Neurosci. 7, 207–219.
[2] Valente, E.M. et al. (2004) Hereditary early-onset Parkinson's disease caused by mutations in PINK1. Science 304, 1158–1160.
[3] Clark, I.E. et al. (2006) Drosophila pink1 is required for mitochondrial function and interacts genetically with parkin. Nature 441, 1162–1166.
[4] Park, J. et al. (2006) Mitochondrial dysfunction in Drosophila PINK1 mutants is complemented by parkin. Nature 441, 1157–1161.
[5] Yang, Y., Ouyang, Y., Yang, L., Beal, M.F., McQuibban, A., Vogel, H. and Lu, B. (2008) Pink1 regulates mitochondrial dynamics through interaction with the fission/fusion machinery. Proc. Natl. Acad. Sci. USA 105, 7070–7075.
[6] Twig, G. et al. (2008) Fission and selective fusion govern mitochondrial segregation and elimination by autophagy. EMBO J. 27, 433–446.
[7] Narendra, D., Tanaka, A., Suen, D.F. and Youle, R.J. (2008) Parkin is recruited selectively to impaired mitochondria and promotes their autophagy. J. Cell Biol. 183, 795–803.
[8] Kim, Y. et al. (2008) PINK1 controls mitochondrial localization of Parkin through direct phosphorylation. Biochem. Biophys. Res. Commun. 377, 975–980.
[9] Vives-Bauza, C. et al. (2010) PINK1-dependent recruitment of Parkin to mitochondria in mitophagy. Proc. Natl. Acad. Sci. USA 107, 378–383.
[10] Kabeya, Y. et al. (2000) LC3, a mammalian homologue of yeast Apg8p, is localized in autophagosome membranes after processing. EMBO J. 19, 5720–5728.
[11] Hatano, T., Kubo, S., Imai, S., Maeda, M., Ishikawa, K., Mizuno, Y. and Hattori, N. (2007) Leucine-rich repeat kinase 2 associates with lipid rafts. Hum. Mol. Genet. 16, 678–690.
[12] Dagda, R.K., Cherra 3rd, S.J., Kulich, S.M., Tandon, A., Park, D. and Chu, C.T. (2009) Loss of PINK1 function promotes mitophagy through effects on oxidative stress and mitochondrial fission. J. Biol. Chem. 284, 13843–13855.
[13] Silvestri, L., Caputo, V., Bellacchio, E., Atorino, L., Dallapiccola, B., Valente, E.M. and Casari, G. (2005) Mitochondrial import and enzymatic activity of PINK1 mutants associated to recessive parkinsonism. Hum. Mol. Genet. 14, 3477–3492.
[14] Beilina, A., Van Der Brug, M., Ahmad, R., Kesavapany, S., Miller, D.W., Petsko, G.A. and Cookson, M.R. (2005) Mutations in PTEN-induced putative kinase 1 associated with recessive parkinsonism have differential effects on protein stability. Proc. Natl. Acad. Sci. USA 102, 5703–5708.
[15] Um, J.W., Stichel-Gunkel, C., Lubbert, H., Lee, G. and Chung, K.C. (2009) Molecular interaction between parkin and PINK1 in mammalian neuronal cells. Mol. Cell Neurosci. 40, 421–432.
[16] Hatano, Y. et al. (2004) Novel PINK1 mutations in early-onset parkinsonism. Ann. Neurol. 56, 424–427.
[17] Sim, C.H., Lio, D.S., Mok, S.S., Masters, C.L., Hill, A.F., Culvenor, J.G. and Cheng, H.C. (2006) C-terminal truncation and Parkinson's disease-associated mutations down-regulate the protein serine/threonine kinase activity of PTEN-induced kinase-1. Hum. Mol. Genet. 15, 3251–3262.
[18] Exner, N. et al. (2007) Loss-of-function of human PINK1 results in mitochondrial pathology and can be rescued by parkin. J. Neurosci. 27, 12413–12418.
[19] Petit, A. et al. (2005) Wild-type PINK1 prevents basal and induced neuronal apoptosis, a protective effect abrogated by Parkinson disease-related mutations. J. Biol. Chem. 280, 34025–34032.
[20] Pridgeon, J.W., Olzmann, J.A., Chin, L.S. and Li, L. (2007) PINK1 protects against oxidative stress by phosphorylating mitochondrial chaperone TRAP1. PLoS Biol. 5, e172.

Cell Death and Differentiation (2007) 14, 887–894

www.nature.com/cdd

Review

Constitutive autophagy: vital role in clearance of unfavorable proteins in neurons

M Komatsu[1,2,3], T Ueno[1], S Waguri[4], Y Uchiyama[5], E Kominami[1] and K Tanaka*[,2]

Investigations pursued during the last decade on neurodegenerative diseases have revealed a common mechanism underlying the development of such diseases: conformational disorder of certain proteins leads to the formation of misfolded protein oligomers, which subsequently develop into large protein aggregates. These aggregates entangle other denatured proteins and lipids to form disease-specific inclusion bodies. The failure of the ubiquitin-proteasome system to shred the protein aggregates has led investigators to focus their attention to autophagy, a bulk degradative system coupled with lysosomes, which is involved in non-selective shredding of large amounts of cytoplasmic components. Research in this field has demonstrated the accumulation of autophagic vacuoles and intracytoplasmic protein aggregates in patients with various neurodegenerative diseases. Although autophagy fails to degrade large protein aggregates once they are formed in the cytoplasm, drug-induced activation of autophagy is effective in preventing aggregate deposition, indicating that autophagy significantly contributes to the clearance of aggregate-prone proteins. The pivotal role of autophagy in the clearance of aggregate-prone proteins has been confirmed by a deductive approach using a brain-specific autophagy-ablated mouse model. In this review, we discuss the consequences of autophagy deficiency in neurons.
Cell Death and Differentiation (2007) **14**, 887–894. doi:10.1038/sj.cdd.4402120; published online 2 March 2007

Cell proteins exist in a balance between continuous synthesis and degradation. In general, this flow of synthesis and degradation (i.e., turnover) contributes to exertion of cell-type-specific functions and maintenance of cell homeostasis. However, it is not uncommon that living cells are exposed to various environmental stresses, such as oxygen radicals and UV irradiation. Unfortunately, these stresses frequently cause various types of protein injuries that vitiate normal cellular functions or homeostasis and may eventually cause cell death. Prompt elimination of injured harmful proteins, which is particularly important in non-proliferative cells, such as neurons, is totally dependent on proper function of protein catabolic machineries, in which two major sophisticated apparatuses play principal roles. One is the proteasome, which is an elegantly organized multi-protease complex with catalytic activities inside its central proteinaceous chamber. It plays crucial roles in selective degradation of short-lived regulatory proteins as well as proteins with aberrant structures that should be eliminated from the cells.[1] The other apparatus is the lysosome that contains many acidic hydrolases, which are separated from the cytosol by the limiting membrane. In this lysosomal pathway, degradation of plasma membrane proteins and extracellular proteins is mediated by endocytosis, whereas that of cytoplasmic components is achieved through distinct types of autophagic pathways; for example, macroautophagy, microautophagy, and chaperone-mediated autophagy.[2,3]

Macroautophagy (hereafter referred to as autophagy), the major type of autophagy, is the bulk protein degradation pathway associated with marked membrane dynamics. In response to various stimuli, such as starvation (i.e., nutritional step-down) and humoral (trophic) factors (e.g., glucagon and cytokines), an isolation membrane appears promptly in the cytosol, where it gradually elongates to sequestrate cytoplasmic constituents. Subsequently, the edges of the membrane fuse together to form double-membrane structures termed autophagosomes. Autophagosomes rapidly fuse with lysosomes, and their contents engulfed together with the inner membrane are degraded by a variety of lysosomal digestive hydrolases (Figure 1).[4] In addition to the importance of starvation-induced (i.e., adaptive) autophagy equipped as a fundamental survival strategy in all eukaryotic cells, growing lines of evidence point to the importance of basal autophagy that operates constitutively at low rate even under nutrient-rich environment and to its key role in global turnover of cellular components including organelles.

[1]Department of Biochemistry, Juntendo University School of Medicine, Tokyo, Japan; [2]Laboratory of Frontier Science, Tokyo Metropolitan Institute of Medical Science, Tokyo, Japan; [3]PRESTO, Japan Science and Technology Corporation, Kawaguchi, Japan; [4]Department of Anatomy and Histology, Fukushima Medical University School of Medicine, Fukushima, Japan and [5]Department of Cell Biology and Neurosciences, Osaka University Graduate School of Medicine, Osaka, Japan
*Corresponding author: K Tanaka, Laboratory of Frontier Science, Tokyo Metropolitan Institute of Medical Science, Bunkyo-ku, Tokyo 113-8613, Japan.
Tel/Fax: +81 3 3823 2237; E-mail: tanakak@rinshoken.or.jp
Keywords: autophagy; neurodegenerative diseases; ubiquitin; knockout-mice; Atg7
Abbreviations: AD, Alzheimer's disease; APP, amyloid precursor protein; Aβ, beta-amyloid; GFP, green fluorescent protein; HD, Huntington's disease; LC3, microtubule-associated protein 1 light chain 3/MAP1LC3; mTor, mammalian target of rapamycin; PD, Parkinson's disease; PS1, presenilin-1; SDH, succinate dehydrogenase; TCA, tricarboxylic acid
Received 28.11.06; revised 05.2.07; accepted 05.2.07; Edited by E Baehrecke; published online 02.3.07

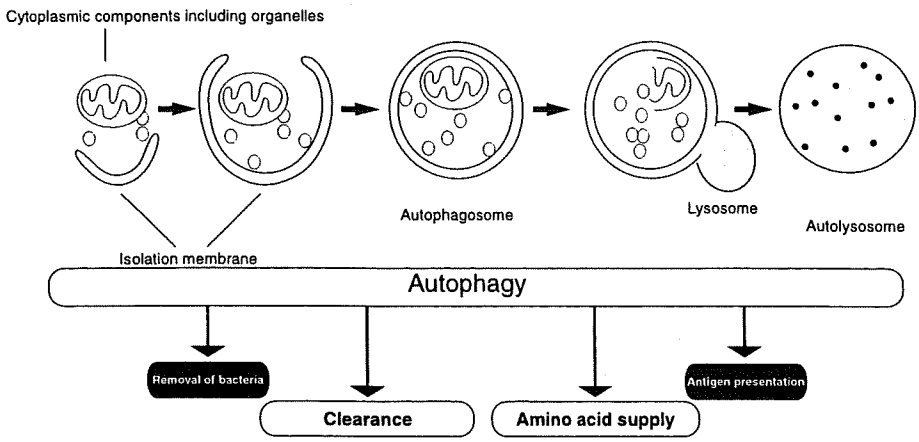

Figure 1 Schematic representation of the physiological functions of autophagy. Autophagy is induced in response to emergency states such as nutrient starvation or bacterial infection, which results in the degradation of cytoplasmic components for amino-acid supply (non-selective process) and the removal of bacteria that invade the cytoplasm (selective process). Autophagy also contributes to processing viral proteins such as EBNA1 and certain cytosolic proteins (e.g., tumor antigens) for presentation onto major histocompatibility complex (MHC) class II molecules. Autophagy also occurs constitutively even under a nutrient-rich state and contributes to global turnover of cellular components. It is an essential cellular process that maintains homeostasis in quiescent cells (e.g., hepatocytes and neurons)

Starvation-induced Autophagy

The most fundamental function of autophagy is cellular adaptation to nutritional stress. In yeast, autophagy is promptly induced upon nitrogen starvation.[5] Transgenic mice overexpressing GFP (green fluorescent protein)-LC3 is an interesting animal model for monitoring autophagy.[6] LC3 (microtubule-associated protein 1 light chain 3/MAP1LC3), originally identified as a small subunit of MAP-1A/MAP-1B, is processed by Atg4B protease to expose the carboxyl-terminal glycine whose residue serves as a donor site for conjugation of target molecules.[7–9] The processed form (LC3-I) undergoes two consecutive ubiquitylation-like modification reactions catalyzed by Atg7 (E1, activating-like enzyme) and Atg3 (E2, conjugating-like enzyme), to be covalently coupled with phosphatidylethanolamine (PE).[10–12] The PE-conjugated form, designated as LC3-II, is then recruited to autophagosomal membrane. Thus, LC3-II is a promising marker for autophagosomal membranes.[7] Similar to endogenous LC3, GFP-LC3 responds to nutrient-starved conditions to form GFP-LC3-II, which is recruited to autophagosomes in GFP-LC3 transgenic mice.[6] The autophagosomal GFP-LC3-II could be detected as dots in fluorescence microscopic analyses. Under fasting conditions, the numbers of fluorescent dots increase in the cytoplasm of the liver, heart, and skeletal muscles of GFP-LC3 transgenic mice.

Starvation-induced protein degradation has been best investigated in the liver. One unequivocal characteristic of hepatic protein degradation is its dependence on the nutrient conditions. Depending on the dietary cycle of the animal, the rate of protein degradation fluctuates between ~1.5% (fed state) and ~4.5% (fasted state) of total liver proteins per hour.[13] Recently, we generated *Atg7*$^{F/F}$:Mx1 mice in which autophagy could be successfully inactivated in the livers.[14] Whereas the amount of total liver proteins decreased to about 66% in the control liver by 1-day fasting, fasting did not result in a significant decrease in the amount of total proteins in the autophagy-deficient liver, indicating that the decrease in total proteins upon fasting is indeed dependent on autophagy. Measurement of the activity of mitochondrial enzyme, succinate dehydrogenase (SDH), showed that fasting was also associated with a significant decrease in SDH activity in total extracts in the control livers, and such reduction was proportional with the decrease in the amount of total protein. On the other hand, fasting was not associated with any change in SDH activity in the autophagy-deficient livers. These results suggest that the mitochondria and cytoplasmic proteins are proportionally degraded upon fasting by autophagy. Thus, it is plausible that autophagosomes surround cytoplasmic components including mitochondria at random to adapt for starvation.

Yeast deficient in autophagy rapidly dies under nutrition-poor conditions,[15] suggesting the important roles of autophagy in maintaining nutrient supply. Indeed, newborn mice deficient in Atg5 or Atg7, which are indispensable for autophagosome formation, show poor response to starvation with regard to production of amino acids, and die within the first day of life.[14,16] Furthermore, Lum *et al.*[17] reported that in IL-3-dependent cells, which cannot undergo apoptosis due to knockout of both Bax and Bak, impairment of autophagy leads to rapid cell death by loss of IL-3, and such death is suppressed by addition of methylpyruvate, a TCA (tricarboxylic acid) substrate. These results suggest that one of the important roles of autophagy is the supply of amino acids under nutrient-poor environment (Figure 2, top panel).

Unique Features of Neuronal Autophagy

The brain appears to be a specially protected tissue where nutrients (e.g., amino acids, glucose, and ketone bodies) are compensated by constant supply from other organs even under starvation conditions and consequently autophagy does not operate in response to nutritional stress. Indeed, autophagosomes-related GFP-LC3 dots do not increase at all

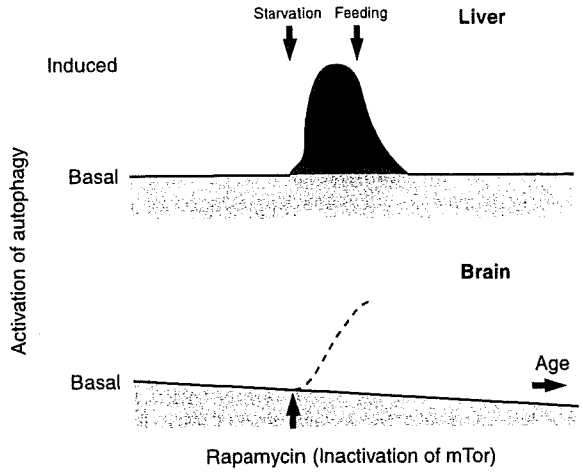

Figure 2 Schematic presentation of induced autophagy and basal (constitutive) autophagy. Under nutrient-rich conditions, autophagic proteolysis proceeds in hepatocytes at a basal rate (top panel, pink zone), which is enhanced two- to threefold to an induced rate under nutrient-starvation conditions (blue zone). When animals are re-fed, the rate of autophagic proteolysis promptly returns to the basal level. In contrast to the liver, autophagy in the brain is thought to proceed at a basal rate, irrespective of nutrient conditions. However, this basal or constitutive autophagy plays a critical role in the quality control system of neurons. Rapamycin and its homologs, which upregulate autophagy to an induced level (bottom panel, broken line), are expected to prevent the accumulation of aggregate-prone proteins. It should be noted that autophagic activity declines with age, which may relate to the age-dependent onset of neurodegenerative diseases

in the brain of GFP-LC3 transgenic mice, irrespective of fasting.[6] A reasonable conclusion drawn from these observations is that autophagy in the brain proceeds at a basal rate but is not enhanced under fasting conditions (Figure 2, bottom panel). Another peculiar feature of autophagy in neurons is the free localization of autophagosomes in the cytoplasm but the restriction of lysosomes mainly to the juxtanuclear cytoplasm of the cell body in the neuron. This feature means that autophagosomes formed in dendrites and synaptic terminal regions must be transported to the lysosome in the cell body. A previous kinetic analysis of organelle movements in cultured neurons indicated that phase-dense vesicles, containing sequestered cytoplasmic proteins and materials taken up by endocytosis, move along microtubules in the axon to the lysosomes in the cell body.[18] These data suggest that fusion of autophagosomes formed in the synaptic cytoplasm with lysosomes is strictly dependent on retrograde axonal transport. It has been reported that mutations of dynein and dynactin in mice and human cause motor neuron degeneration resembling amyotrophic lateral sclerosis.[19,20] Using cultured PC12 cells, flies and mice expressing different kinds of aggregate-prone proteins, such as expanded polyQ and mutant α-synuclein, Ravikumar *et al.*[21] demonstrated that inhibition of dynein function retarded the clearance of aggregates by inhibiting autophagosome-lysosome fusion. It has been shown recently that aggregate-prone proteins formed in the cytoplasm of cultured HeLa cells and a cultured neural cell line, are degraded by autophagy, which is also dependent on intact microtubules.[22]

Autophagic Vacuoles in Neurodegenerative Diseases

Morphological analyses revealed that accumulation of abnormally large number of autophagic vacuoles (autophagosomes plus autolysosomes) or the appearance of irregularly shaped autophagic vacuoles is frequently observed as a common feature in many inherited neurodegenerative diseases.[23–27] Inclusion bodies, composed of ubiquitin-positive cytoplasmic remnants, and lipofuscin deposits, together with dispersed autophagic vacuoles and lysosomes are the primary hallmarks of the late stages of these diseases. Increased density of autophagic vacuoles seems to reflect enhanced autophagosome formation, on one hand, but their accumulation with blurred structures of sequestered materials in their lumen may also imply impaired autolysosomal degradation, on the other. In fact, these morphological features are not present in normal neurons and resemble those of cultured HEK293 cells that have been placed under starvation conditions in the presence of lysosomal proteinase inhibitors.[28] Under these conditions, autophagic response is markedly enhanced, but autophagic proteolysis is simultaneously inhibited. In addition, as observed in Danon disease, which is caused by mutation of the lysosome-associated membrane protein-2 (LAMP-2), and LAMP-2-deficient mice, impairment of autophagosome-lysosome fusion also leads to unequivocal increment of autophagosomes in cardiac muscles and hepatocytes.[29,30]

Autophagy in Alzheimer's, Huntington's, and Parkinson's Diseases

Protein conformational disorders, such as Alzheimer's disease (AD), Huntington's disease (HD), and Parkinson's disease (PD), are characterized by abnormally high accumulation of misfolded and/or unfolded proteins in the surviving neurons as detected at postmortem examination. In this section, we will evaluate the role of autophagy in those hereditary neurodegenerative diseases.

It has become clear that autophagy is linked to the pathogenesis of HD. HD is an autosomal dominant disorder caused by mutations of huntingtin, a cytosolic protein that has a polyglutamine (polyQ) tract in its N-terminus. In HD, abnormal expansion of polyQ caused by codon (CAG) reiterations in exon 1 of the Huntingtin gene produces mutated huntingtin with an expanded polyQ repeat (more than 37 polyQs). Mutant huntingtin with a longer polyQ tract has a stronger tendency than the wild type to form aggregates, both accelerating the onset and worsening the severity of the disease, suggesting that the progressive formation of insoluble polyQ aggregates is a key event leading to manifestation of the disease. Indeed, model mouse with mutant polyQ is associated with formation of nuclear and cytoplasmic inclusions in their neurons.[31] However, recent studies revealed that globular and protofibrillar intermediates form before the organization of mature huntingtin aggregates, and that these are toxic and could lead to disturbances of genetic transcription networks and mitochondrial dysfunctions.[32,33] Then, what are the mechanisms by which autophagy clears mutant huntingtin? Ultrastructural examination of huntingtin-transfected cells showed abundant accumulation of cathepsin

D-positive autophagic vacuoles with or without sequestered cellular constituents, dense lysosomes, and multilamellar and tubuloveseicular structures.[26] Ravikumar *et al.*[34] investigated whether autophagy can degrade mutant huntingtin with expanded polyQ repeats. Degradation of 74 polyQ repeats fused to the amino terminus of GFP (polyQ74-GFP) transfected into COS7 or PC12 cells was inhibited by 3-methyladenine, a specific inhibitor of autophagy, and enhanced by rapamycin. Rapamycin acts by inhibiting the mammalian target of rapamycin (mTor) kinase, which forms the core of a nutrient- and growth factor-sensitive complex that control protein synthesis, and suppresses autophagy.[35] Importantly, inhibitors of autophagy enhance cell death, whereas rapamycin prevents the effects. Furthermore, once the overexpressed polyQ74-GFP forms insoluble large aggregates, the insoluble aggregates become resistant to rapamycin-induced autophagy. The data clearly demonstrate that failure to degrade polyQ expansions by autophagy is associated with accelerated progression of HD and that stimulation of autophagy in the early stages of the disease by rapamycin treatment could prevent deposition of polyQ aggregates. Rapamycin enhances the autophagic clearance of different proteins with long polyQ and polyalanine (polyA)-expanded proteins, and reduces their neurotoxicity. Thus, rapamycin and its analogs can be potentially used therapeutically for neurodegenerative diseases caused by aggregate-prone proteins.[36] It has been shown that mTor is sequestered in polyQ aggregates in transgenic mice expressing mutant huntingtin and patient brains of HD. Sequestration of mTor in polyQ aggregates inhibits nuclear-cytoplasm shuttling of mTor, leading to inactivation of mTor.[37] The inactivation in turn induces autophagy. Hence, co-sequestration of aggregates with mTor leads to inhibition of mTor activity, which may provide a partial explanation for accumulation of autophagic vacuoles in neurodegenerative diseases. On the other hand, the activation of autophagy via an insulin signal pathway clears accumulated polyQ proteins independent of mTor, as reported by Yamamoto *et al.*[38] They found that aggregates of mutant huntingtin activate insulin receptor substrate-2 involving the signaling cascades of insulin and insulin-like growth factor 1. Such activation turns on class III PI3K to induce autophagy, thus contributing to clearance of huntingtin aggregates.[38]

Invariably, AD is the most prevalent form of neurodegenerative diseases with dementia and associates with extracellular deposition of beta-amyloid (Aβ). Presenilin-1 (PS1) is one of several proteins linked to early-onset familial AD, and together with PS2, plays a catalytic role in the γ-secretase complex necessary for intermediate proteolysis of the amyloid precursor protein (APP) followed by liberation of Aβ. Although it has been noticed that autophagic vacuoles accumulate in hippocampal and prefrontal cortical pyramidal neurons of Alzheimer-type dementia,[23,24] the mechanism remains unclear. Wilson *et al.*[39] found the formation of enlarged late endosome-like structures, including α- and β-synuclein, in the perikarya of PS1$^{-/-}$ primary neurons and hippocampal tissue of patients with the Levy body variant of AD. Formation of such organelles is rescued by exogenous expression of not only wild-type PS but also dominant-negative PS1 lacking its activity, indicating that PS1 has another function besides γ-secretase. Esselens *et al.*[40] demonstrated the accumulation of telencephalin, a neural specific intercellular adhesion molecule known to interact with PS1, in vacuoles positive for Atg12 and LC3, but not cathepsin D, in PS1$^{-/-}$ hippocampal neurons. Similar to the report of Wilson *et al*,[39] the formation of such vacuoles was suppressed by not only wild-type but also mutant PS1. Furthermore, Esselens *et al.*[40] used cathepsin D knockout mice to show the degradation of telencephalin in lysosomes. Collectively, these results suggest that PS1 might play important roles in autophagosome and lysosomal fusion step. Recently, Yu *et al.*[41] reported the role of autophagy in Aβ production. Their exhaustive electron and immunoelectron microscopic analyses revealed accumulation of LC3-positive autophagic vacuoles in brains of AD patients and in AD model mice, neural cell lines, and in a non-neural APP-expressing cell line, and also the localization of PS1, Aβ40, Aβ42, and necastrin on internal and limiting membrane components of autophagic vacuoles. Further, they found that induction of autophagy evoked Aβ production, and inversely, inhibition of autophagy suppressed Aβ production. Finally, they observed the PS1-dependent γ-secretase activity in biochemical isolated autophagic vacuoles. Based on these findings, they proposed a novel mechanism for the generation of Aβ via autophagy that emphasized the prominent role of autophagy in AD pathogenesis.[41]

PD is a neurodegenerative disorder associated with progressive loss of dopaminergic neurons of the substantia nigra and locus coeruleus. The major clinical symptoms of PD are body rigidity, hypokinesia, and postural instability associated with trembling extremities.[42] Pathological examination shows marked accumulation of cytoplasmic inclusions of proteinaceous material with lipids called Lewy bodies. Lewy bodies consist of lipids, ubiquitin, enzymes involved in ubiquitin-related pathways, neurofilament proteins, α-synuclein, synphilin-1, and other entangled proteins. Mutations in the gene encoding α-synuclein, which is localized in presynaptic terminals and is abundantly present in Lewy bodies, are identified in certain cases of familial PD.[43,44] α-Synuclein is a protein of unknown function and a major component of Lewy bodies. Among three point mutations in α-synuclein causing an autosomal dominant form of familial PD, two mutations of α-synuclein (A53T and A30P) have been studied extensively. These α-synuclein mutants have a stronger tendency to form fibrils than wild-type α-synuclein. Hence, similar to huntingtin with abnormal polyQ expansion, misfolded or aggregated α-synuclein is believed to cause cell toxicity and inhibits the ubiquitin-proteasome system. Lewy bodies may contribute to aggregation of α-synuclein into inclusions to moderate its toxicity.[45,46] It has been reported recently that autophagic-lysosomal dysfunction may be also involved in PD. Using stable PC12 transfectants expressing wild-type and A53T mutant α-synuclein, Stefanis *et al.*[47] showed that marked accumulation of autophagic vacuoles and impairment of lysosomal and ubiquitin-proteasome functions are principal phenotypes in the cells. On the other hand, clearance of mutant α-synuclein is strongly dependent on both ubiquitin-proteasomes and macroautophagy,[48] but not chaperone-mediated autophagy capable of degrading wild-type α-synuclein efficiently.[49]

Impairment of Autophagy in Neurons

Recently, our group and Mizushima's group investigated the pathophysiological roles of basal or constitutive autophagy in the brain.[50,51] For this purpose, we generated neuron-specific autophagy-deficient mice (*Atg7*$^{F/F}$:Nes mice) by crossing *Atg7*-conditional knockout mice (*Atg7*$^{F/F}$) with transgenic mice expressing the Cre recombinase under the control of the neuron-specific Nestin (Nes) promoter, Nes-*Cre*. We found that mice lacking Atg7 (i.e., autophagy) in the central nervous system exhibited various behavioral deficits, such as abnormal limb-clasping reflexes and reduction of coordinated movement, and died within 28 weeks after birth. Histological analysis showed that *Atg7*-deficiency was associated with neuronal loss in the cerebral and cerebellar cortices. Intriguingly, *Atg7*-deficient neurons showed abundant accumulation of polyubiquitylated proteins, which appeared as inclusion bodies whose size and number increased with aging (Figure 3), but had functionally intact proteasomes, whose impairment is generally known to cause abnormal ubiquitin-mediated proteolysis.[50] Hara *et al*.[51] also reported that almost all these phenotypes, if not all, were observed in neural-specific mice deficient in *Atg5*, another autophagy-essential gene. Thus, many of the critical symptoms seen in neural-specific autophagy-deficient mice are similar to those of patients with neurodegenerative disorders.

Histological analyses of the brains of *Atg7*$^{F/F}$:Nes mice revealed loss of specific neurons, such as pyramidal neurons in the cerebral cortex and hippocampus, and Purkinje cells in the cerebellum. Unexpectedly, immunohistological analysis using anti-ubiquitin antibody identified ubiquitin-positive proteinaceous aggregates throughout the brain, although the staining intensity varied from one region to another. Few ubiquitin-positive inclusions were recognized in brain regions with evident neuronal loss, whereas many ubiquitin inclusions were noted in areas with barely any neuronal loss such as the hypothalamus. Although we could not determine whether neuronal death is due to accumulation and subsequent inclusion formation of ubiquitylated proteins, neurons with large inclusions survived. Conversely, large pyramidal neurons and Purkinje cells seem vulnerable to ubiquitylated proteins and die before the formation of large inclusions. Whether the formation of inclusion bodies in neurons is protective or toxic is under debate, although emerging evidence emphasizes that protein aggregation can be a protective mechanism.[32,33]

Although accumulation of ubiquitylated proteins and cell death were noted in autophagy-deficient hepatocytes[14] and neurons,[50,51] such phenotypes were not observed in growing cells such as mouse embryonic fibroblasts (MEFs) and astroglial cells, irrespective of autophagy deficiency. Thus, it seems that autophagy is not required in rapidly dividing cells, at least with respect to multiplication of these cells. These results might also reflect the difference in autophagic activity among cell types. It is possible that the cell division cycle results in dilution of ubiquitylated proteins in autophagy-deficient MEFs, preventing their accumulation. Alternatively, other degradation pathways, such as chaperone-mediated autophagy, could contribute to degradation of long-lived proteins in growing MEFs. Considered together, it is clear that macroautophagy (the massive autophagy pathway discussed here) plays important roles in proteolysis in quiescent cells.

Autophagy deficiency is considered to result in delays of global turnover of cytoplasmic components, resulting in accumulation of misfolded and/or unfolded proteins followed by formation of inclusion bodies. However, a recent report showed that p62/SQSTM1 harboring a ubiquitin binding domain, interacted with LC3 and was degraded via autophagy.[52] We also obtained similar results and found that

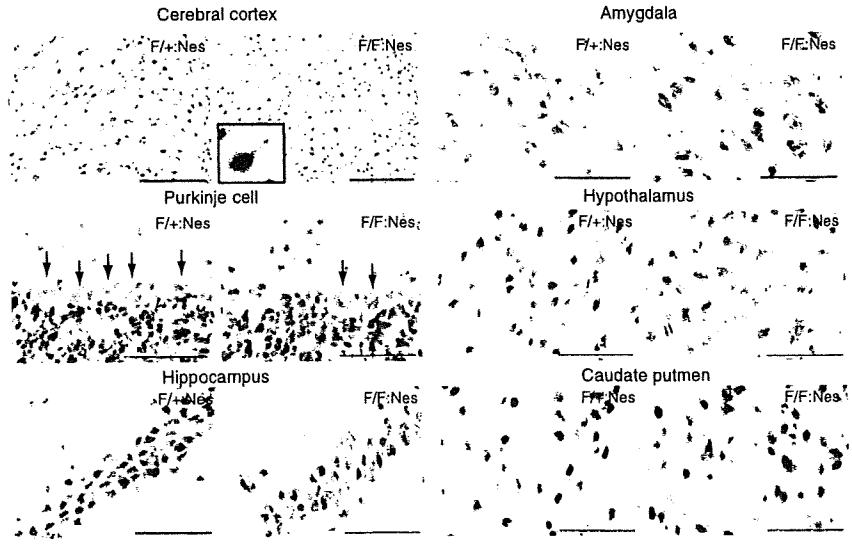

Figure 3 Ubiquitin-positive inclusions in autophagy-deficient neurons. The presence of ubiquitin-positive dots was examined immunohistochemically in several regions of the brain including cerebral cortex, cerebellum (Purkinje cells), hippocampus, amygdala, hypothalamus, caudate putamen of *Atg7*$^{F/+}$:Nes (left panels), and *Atg7*$^{F/F}$:Nes (right panels) mice. Note the presence of numerous ubiquitin dots in the amygdala and hypothalamus of representative mutants. Bars, 100 μm in the panel of cerebral cortex, and 50 μm in others

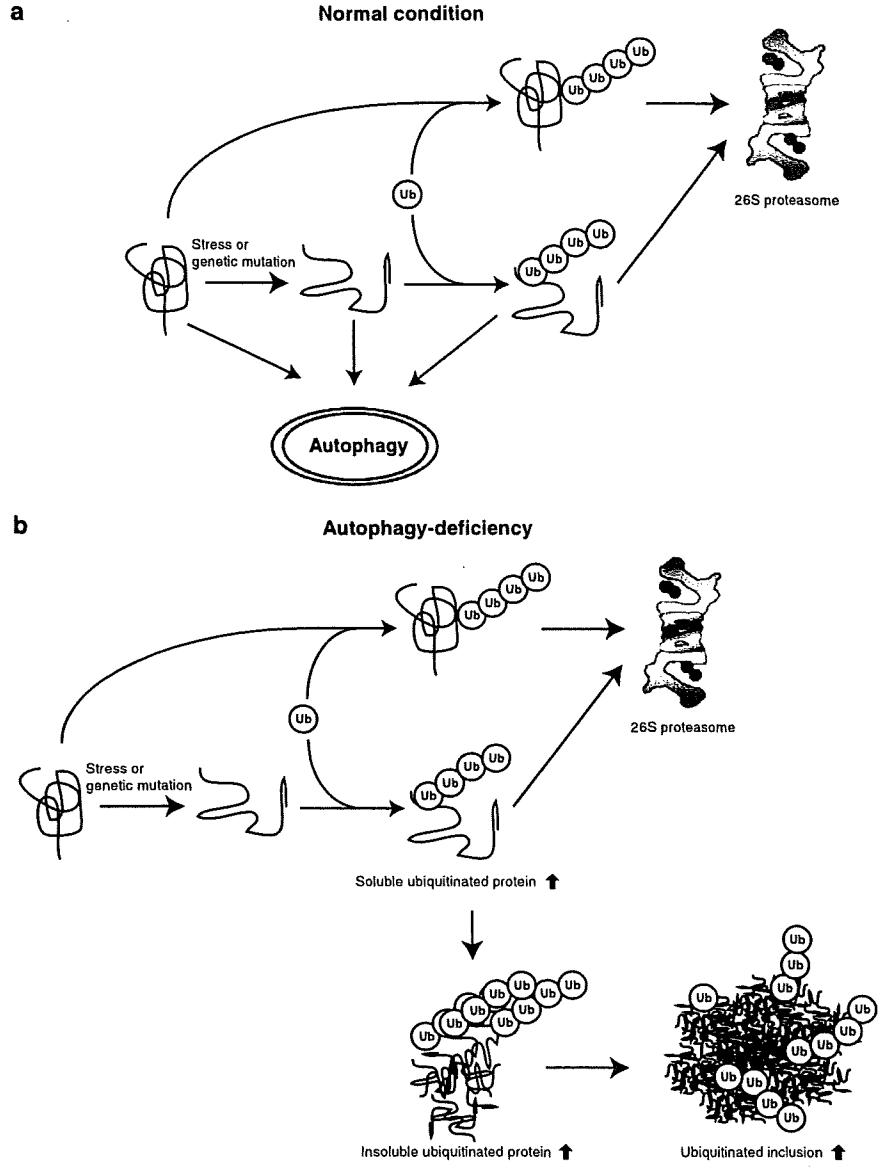

Figure 4 A schematic diagram of protein destruction pathways mediated by the proteasome and autophagy. The majority of cellular proteins, if not all, are polyubiquitylated before hydrolysis by the proteasome (an ATP-dependent proteolytic complex). Similarly, unfolded/misfolded proteins generated by environmental stresses or genetic mutations are discarded after polyubiquitylation by the same proteolytic system (**a**). Aging-related decline in autophagic activity causes accumulation of highly ubiquitylated proteins, which are recovered as both soluble and insoluble forms (**b**). As autophagy could feed both ubiquitylated and unubiquitylated protein(s), it is not clear at present whether polyubiquitylated aggregates/inclusions in autophagy-deficient neurons are formed consequent to impairment of degradation of unubiquitylated proteins or aggressively polyubiquitylated proteins. In addition, further work is needed to determine whether the two proteolytic systems (autophagy and proteasomes) work independently or cooperatively, and whether autophagy and the proteasome feed a similar set of normal and/or misfolded/unfolded proteins in general. Red text: protein dynamics associated with autophagy deficiency, Ub: ubiquitin

p62 plays a critical role in the formation of ubiquitin-positive aggregates by impaired autophagy (unpublished data). These results imply that ubiquitylated unfavorable proteins might be selectively sequestered into autophagosomes in part via p62 (which may retain its shuttling ability of ubiquitylated proteins). In either case (non-selective or selective degradation of ubiquitylated proteins by autophagy), our results indicate that autophagy operates not only as a supplier of amino acids under nutrient-poor conditions but also as a house cleaner of damaged proteins under nutrient-rich conditions.

Concluding Remarks

Considering the role of autophagy in neurodegenerative diseases, it is possible to align time-dependent enhancement and inactivation of autophagy. First, misfolded and/or

unfolded protein aggregates formed in neurons cause sequestration of mTor along with the aggregates, leading to significant inactivation of mTor, which stimulates autophagy (autophagosome formation). Second, if the size of aggregates is small enough and the degree of aggregation is moderate, the aggregates are engulfed into autophagosomal lumen and subsequently degraded via autophagy. Unless the amounts of aggregates surpass the clearance capacity of autophagosomes, maximal activation of autophagy by pharmaceutical agents such as rapamycin could be effective in preventing the progression of the disease. It is noteworthy that the expression of aggregation-prone protein(s) observed frequently in familial neurodegenerative disorders is not required for the formation of inclusions associated with impaired autophagy, suggesting the involvement of autophagy even in sporadic neurodegenerative diseases. On the other hand, autophagic activity of rat liver decreases with aging and this decrease conversely correlates with an increase in the accumulation of oxidized proteins.[36] Thus, age-dependent onset of neurodegenerative diseases most likely correlates with the age-dependent decline of autophagic activity. It is generally accepted that deficits of the proteasome-ubiquitin system are linked to various neurodegenerative disorders. Intriguingly, however, no obvious inhibition of the ubiquitin-proteasome system occurs in the mouse brain lacking autophagy, providing compelling evidence that constitutive autophagy plays a prominent role in neuronal survival, independent of proteasome function (Figure 4). In this context, we stress that proteasome inhibition induces augmented autophagy in order to eliminate unnecessary accumulated proteins, probably compensating the loss of proteasome functions.[22] Thus, the two major proteolytic pathways naturally differ in the cooperative responses in cells. We emphasize the importance of autophagy as a process with adaptive and flexible responses. Finally, a better understanding of basal or constitutive autophagy, which maintains basal activity of macroautophagy in neurons, may help in the design of new strategies to prevent neurodegenerative diseases.

1. Goldberg AL. Protein degradation and protection against misfolded or damaged proteins. *Nature* 2003; **426**: 895–899.
2. Levine B, Klionsky DJ. Development by self-digestion: molecular mechanisms and biological functions of autophagy. *Dev Cell* 2004; **6**: 463–477.
3. Cuervo AM. Autophagy: in sickness and in health. *Trends Cell Biol* 2004; **14**: 70–77.
4. Mizushima N, Ohsumi Y, Yoshimori T. Autophagosome formation in mammalian cells. *Cell Struct Funct* 2002; **27**: 421–429.
5. Takeshige K, Baba M, Tsuboi S, Noda T, Ohsumi Y. Autophagy in yeast demonstrated with proteinase-deficient mutants and conditions for its induction. *J Cell Biol* 1992; **119**: 301–311.
6. Mizushima N, Yamamoto A, Matsui M, Yoshimori T, Ohsumi Y. *In vivo* analysis of autophagy in response to nutrient starvation using transgenic mice expressing a fluorescent autophagosome marker. *Mol Biol Cell* 2004; **15**: 1101–1111.
7. Kabeya Y, Mizushima N, Ueno T, Yamamoto A, Kirisako T, Noda T *et al.* LC3, a mammalian homologue of yeast Apg8p, is localized in autophagosome membranes after processing. *EMBO J* 2000; **19**: 5720–5728.
8. Kabeya Y, Mizushima N, Yamamoto A, Oshitani-Okamoto S, Ohsumi Y, Yoshimori T. LC3, GABARAP and GATE16 localize to autophagosomal membrane depending on form-II formation. *J Cell Sci* 2004; **117**: 2805–2812.
9. Tanida I, Sou YS, Ezaki J, Minematsu-Ikeguchi N, Ueno T, Kominami E. HsAtg4B/HsApg4B/autophagin-1 cleaves the carboxyl termini of three human Atg8 homologues and delipidates microtubule-associated protein light chain 3- and GABAA receptor-associated protein-phospholipid conjugates. *J Biol Chem* 2004; **279**: 36268–36276.
10. Ichimura Y, Kirisako T, Takao T, Satomi Y, Shimonishi Y, Ishihara N *et al.* A ubiquitin-like system mediates protein lipidation. *Nature* 2000; **408**: 488–492.
11. Tanida I, Tanida-Miyake E, Ueno T, Kominami E. The human homolog of Saccharomyces cerevisiae Apg7p is a Protein-activating enzyme for multiple substrates including human Apg12p, GATE-16, GABARAP, and MAP-LC3. *J Biol Chem* 2001; **276**: 1701–1706.
12. Tanida I, Tanida-Miyake E, Komatsu M, Ueno T, Kominami E. Human Apg3p/Aut1p homologue is an authentic E2 enzyme for multiple substrates, GATE-16, GABARAP, and MAP-LC3, and facilitates the conjugation of hApg12p to hApg5p. *J Biol Chem* 2002; **277**: 13739–13744.
13. Mortimore GE, Hutson NJ, Surmacz CA. Quantitative correlation between proteolysis and macro- and microautophagy in mouse hepatocytes during starvation and refeeding. *Proc Natl Acad Sci USA* 1993; **80**: 2179–2183.
14. Komatsu M, Waguri S, Ueno T, Iwata J, Murata S, Tanida I *et al.* Impairment of starvation-induced and constitutive autophagy in Atg7-deficient mice. *J Cell Biol* 2005; **169**: 425–434.
15. Tsukada M, Ohsumi Y. Isolation and characterization of autophagy-defective mutants of Saccharomyces cerevisiae. *FEBS Lett* 1993; **333**: 169–174.
16. Kuma A, Hatano M, Matsui M, Yamamoto A, Nakaya H, Yoshimori T *et al.* The role of autophagy during the early neonatal starvation period. *Nature* 2004; **432**: 1032–1036.
17. Lum JJ, Bauer DE, Kong M, Harris MH, Li C, Lindsten T *et al.* Growth factor regulation of autophagy and cell survival in the absence of apoptosis. *Cell* 2005; **120**: 237–248.
18. Hollenbeck PJ. Products of endocytosis and autophagy are retrieved from axons by regulated retrograde organelle transport. *J Cell Biol* 1993; **121**: 305–315.
19. Puls I, Jonnakuty C, LaMonte BH, Holzbaur EL, Tokito M, Mann E *et al.* Mutant dynactin in motor neuron disease. *Nat Genet* 2003; **33**: 455–456.
20. Hafezparast M, Klocke R, Ruhrberg C, Marquardt A, Ahmad-Annuar A, Bowen S *et al.* Mutations in dynein link motor neuron degeneration to defects in retrograde transport. *Science* 2003; **300**: 808–812.
21. Ravikumar B, Acevedo-Arozena A, Imarisio S, Berger Z, Vacher C, O'Kane CJ *et al.* Dynein mutations impair autophagic clearance of aggregate-prone proteins. *Nat Genet* 2005; **37**: 771–776.
22. Iwata A, Riley BE, Johnston JA, Kopito RR. HDAC6 and microtubules are required for autophagic degradation of aggregated huntingtin. *J Biol Chem* 2005; **280**: 40282–40292.
23. Okamoto K, Hirai S, Iizuka T, Yanagisawa T, Watanabe M. Reexamination of granulovacuolar degeneration. *Acta Neuropathol (Berlin)* 1991; **82**: 340–345.
24. Cataldo AM, Hamilton DJ, Barnett JL, Paskevich PA, Nixon RA. Properties of the endosomal-lysosomal system in the human central nervous system: disturbances mark most neurons in populations at risk to degenerate in Alzheimer's disease. *J Neurosci* 1996; **16**: 186–199.
25. Anglade P, Vyas S, Javoy-Agid F, Herrero MT, Michel PP, Marquez J *et al.* Apoptosis and autophagy in nigral neurons of patients with Parkinson's disease. *Histol Histopathol* 1997; **12**: 25–31.
26. Kegel KB, Kim M, Sapp E, McIntyre C, Castano JG, Aronin N *et al.* Huntingtin expression stimulates endosomal-lysosomal activity, endosome tubulation, and autophagy. *J Neurosci* 2000; **20**: 7268–7278.
27. Petersen A, Larsen KE, Behr GG, Romero N, Przedborski S, Brundin P *et al.* Expanded CAG repeats in exon 1 of the Huntington's disease gene stimulate dopamine-mediated striatal neuron autophagy and degeneration. *Hum Mol Genet* 2001; **10**: 1243–1254.
28. Tanida I, Minematsu-Ikeguchi N, Ueno T, Kominami E. Lysosomal turnover, but not a cellular level, of endogenous LC3 is a marker for autophagy. *Autophagy* 2005; **1**: 84–91.
29. Nishino I, Fu J, Tanji K, Yamada T, Shimojo S, Koori T *et al.* Primary LAMP-2 deficiency causes X-linked vacuolar cardiomyopathy and myopathy (Danon disease). *Nature* 2000; **406**: 906–910.
30. Tanaka Y, Guhde G, Suter A, Eskelinen EL, Hartmann D, Lullmann-Rauch R *et al.* Accumulation of autophagic vacuoles and cardiomyopathy in LAMP-2-deficient mice. *Nature* 2000; **406**: 902–906.
31. Ikeda H, Yamaguchi M, Sugai S, Aze Y, Narumiya S, Kakizuka A. Expanded polyglutamine in the Machado–Joseph disease protein induces cell death *in vitro* and *in vivo*. *Nat Genet* 1996; **13**: 196–202.
32. Sanchez I, Mahlke C, Yuan J. Pivotal role of oligomerization in expanded polyglutamine neurodegenerative disorders. *Nature* 2003; **421**: 373–379.
33. Arrasate M, Mitra S, Schweitzer ES, Segal MR, Finkbeiner S. Inclusion body formation reduces levels of mutant huntingtin and the risk of neuronal death. *Nature* 2004; **431**: 805–810.
34. Ravikumar B, Duden R, Rubinsztein DC. Aggregate-prone proteins with polyglutamine and polyalanine expansions are degraded by autophagy. *Hum Mol Genet* 2002; **11**: 1107–1117.
35. Inoki K, Corradetti MN, Guan KL. Dysregulation of the TSC-mTOR pathway in human disease. *Nat Genet* 2005; **37**: 19–24.
36. Bergamini E. Autophagy: a cell repair mechanism that retards ageing and age-associated diseases and can be intensified pharmacologically. *Mol Aspects Med* 2006; **27**: 403–410.
37. Ravikumar B, Vacher C, Berger Z, Davies JE, Luo S, Oroz LG *et al.* Inhibition of mTOR induces autophagy and reduces toxicity of polyglutamine expansions in fly and mouse models of Huntington disease. *Nat Genet* 2004; **36**: 585–595.
38. Yamamoto A, Cremona ML, Rothman JE. Autophagy-mediated clearance of huntingtin aggregates triggered by the insulin-signaling pathway. *J Cell Biol* 2006; **172**: 719–731.
39. Wilson CA, Murphy DD, Giasson BI, Zhang B, Trojanowski JQ, Lee VM. Degradative organelles containing mislocalized alpha-and beta-synuclein proliferate in presenilin-1 null neurons. *J Cell Biol* 2004; **165**: 335–346.